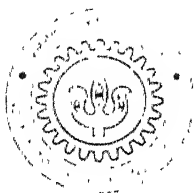


HYDROTHERMAL SYNTHESIS OF Gd_2O_3 STABILIZED ZIRCONIA POWDERS

Animesh Kundu

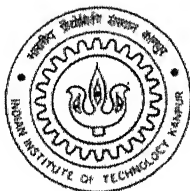
TH
msp/2001/m
K



MATERIALS SCIENCE PROGRAMME
INDIAN INSTITUTE OF TECHNOLOGY KANPUR
KANPUR
UP 208016
INDIA

HYDROTHERMAL SYNTHESIS OF Gd_2O_3 STABILIZED ZIRCONIA POWDERS

Animesh Kundu



MATERIALS SCIENCE PROGRAMME
INDIAN INSTITUTE OF TECHNOLOGY KANPUR
KANPUR
UP 208016
INDIA

9 FEB 2003 / MSP

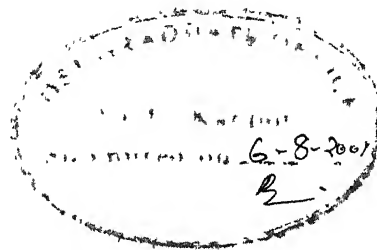
पुरुषोत्तम काशीनाथ निरंकर पुस्तकालय

भारतीय प्रौद्योगिकी संस्थान कानपुर

अवधि क्र० A-----
141850

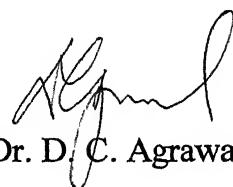


A111850



CERTIFICATE

It is certified that the work contained in this thesis entitled "*Hydrothermal Preparation of Gd_2O_3 Stabilized Zirconia Powders*", by *Animesh Kundu*, has been carried out under my supervision and that this work has not been submitted elsewhere for any degree.



Dr. D. C. Agrawal

Professor

Materials Science Programme,

Indian Institute of Technology, Kanpur

August 2001

Acknowledgement

I would like to thank my supervisor Dr. D. C. Agrawal for introducing me to field of zirconia ceramics and hydrothermal processing. I thank him for his patience, constant encouragement and excellent guidance. During my stay in this institute I have learned many things from him. I am grate to him for his generosity. I wish that he will keep in touch with me in future and will continue to give his valuable advice.

I thank all the staff of the Glass Blowing Workshop for their help and support during the entire course of work. I would also like to thank all the staff of ACMS and MSP for their cooperation. I acknowledge the immense help Mr. Umashankar Singh, Mr. G. S. Thapa, Sardarji, Mr Jaikishan, and Mr. B.Sharma for their constant help in doing the experiments and characterizing the samples throughout last one and half years.

I thank all my lab mates Niraj, Sahooji, Sreya, Aditi, Arpana for maintaining a cordial, collaborative and lively research environment in the lab. It was a nice and memorable association with all of them. In spite of their busy schedule Sandesh and Niraj help me in the final stages of thesis preparation. I thank them again and again.

During this long stay at I.I.T. Kanpur many people helped in different ways and it is not possible to acknowledge each of them in this small space. I thank them all for their help and their cooperation. I am fortunate enough to have friends like Feroz, Ashotosh, Abhishek, Sudha, Rama, Rajrup, Soubhik, Souvik, PP, Argha, Santanu, Sagnik, Subhasish, Debu, Nano, Bala, Rupen, Kaustav, Sandip, Arindum, Sankar, Bharat who made my stay cherishable and a memorable one.

I wish to give a heartfelt thanks to Prof Malay Chaudhuri and his wife for their constant help and support. Kakima's, Mrs Malay Chaudhuri, delicious Bengali dishes always made me feel at home away from home. I thank Sreya for introducing me to them.

The unhesitating help and support rendered by Subhai, Soubhik, Sagnik, Saugata and Amlan at the hour of crisis will be remembered forever.

The unbreakable patience of my family members and their silent support was always a constant source of inspiration.

Animesh Kundu
August 2001

Contents

Abstract.....	i
List of figures	iii
List of tables.....	vi
Hydrothermal preparation of ultrafine powders...	1
1.1. Introduction.....	1
1.2. Mechanism of hydrothermal crystallization.....	5
1.2.1 Hydrothermal crystallization at acidic pH..	5
1.2.2 Hydrothermal crystallization at acidic pH...	7
1.3 Urea hydrolysis.....	13
1.4 Role of washing in the preparation of fine powders.....	15
1.5 Statement of the problem.....	18
2. Experimental Procedure.....	21
2.1 Powder Preparation.....	21
2.1.1. Urea hydrolysis and drying.....	23
2.1.2. Optimization of urea hydrolysis.....	25
2.1.3. Hydrothermal crystallization.....	27
2.1.4. Calculations of the amount of water required to generate the desired pressures.....	29

2.2	Powder characterization.....	32
2.2.1.	X-ray diffraction.	35
2.2.1.1	crystallite size analysis.....	36
2.2.2.	Scanning electron microscopy (sem).....	37
2.2.3.	Bet surface area measurement....	40
2.2.4.	Particle size analysis... ..	41
3.	Results and discussions	42
3.1.	Optimization of the urea hydrolysis process.....	42
3.1.1.	Properties of amorphous powder obtained after urea hydrolysis.....	51
3.2	Hydrothermal crystallization.....	55
3.2.1	Effect of gadolinia content on the hydrothermally crystallized powders.....	60
3.2.2	Effect of hydrothermal treatment pressure.....	63
3.2.3	Effect of high temperature steam-water mixture on the hydrothermal crystallization.....	64
3.2.4	Seeding experiments.....	65
4.	Conclusion	74
	References	77

Abstract

Preparation of stabilized zirconia powders and the development of new stabilized zirconia is a topic of continued research interest. Gadolinia (Gd_2O_3) is an effective stabilizer for zirconia but the preparation of Gd_2O_3 stabilized zirconia powders by conventional techniques is difficult. Furthermore, the techniques such as sol-gel and coprecipitation yield amorphous powders, which have to be calcined at high temperatures for conversion to stabilized crystalline phase. The hydrothermal preparation of powders is capable of directly producing crystalline powders. In the present work Gd_2O_3 doped zirconia powders have been prepared by urea hydrolysis and hydrothermal crystallization. An amorphous powder is first prepared by the urea hydrolysis of a mixed salt solution of zirconium oxychloride and gadolinium nitrate at $\sim 105^\circ\text{C}$ for 6 hours. The coprecipitated powder is washed repeatedly with water and n-propanol and dried at 80°C for 8 hours. The dried powder is subjected to high temperature and pressure existing in a superheated steam or steam- water mixture in a sealed quartz tube. Different temperature, pressure and pH conditions are investigated. The amorphous precursor and the powder obtained after hydrothermal treatment is characterized by scanning electron microscopy, particle size analysis, BET surface area measurement, thermogravimetric analysis, FTIR etc. The amorphous powder has a surface area of $245 \text{ m}^2/\text{gm}$. The amorphous powder can be crystallized at a temperature as low as 220°C , pressure 1.6 MPa, and treatment time 6 hours. With the increase in hydrothermal temperature and pressure the crystallite size as determined from x-ray peak broadening increases, but the overall particle size distribution changes only slightly. Also the particle size varies between $0.1 \mu\text{m}$ and $35 \mu\text{m}$ whereas the

crystallite size is in the range 20 nm to 50nm showing large agglomeration in the powder. The degree of crystallization of the amorphous powder and the crystallite size increases as the hydrothermal pressure is increased at a constant temperature (220°C) and time (6 hours). High temperature steam-water mixture rather than superheated steam is more effective in the crystallization of the amorphous powder. When the hydrothermal treatment was done in steam-water mixture the amorphous powder crystallizes in 2 hours at 220°C compared to 6 hours required at the same temperature when the amorphous powder was crystallized in superheated steam.

Powders containing 2, 5, 8 and 10-mole % Gd_2O_3 were successfully prepared by hydrothermal crystallization at 270°C, 1.8 MPa for 6 hours. The phases obtained were monoclinic ZrO_2 for 2 and 5-mole % Gd_2O_3 and cubic ZrO_2 for 8 and 10 mole % ZrO_2 .

An important issue in the hydrothermal crystallization is the mechanism of nucleation and growth of the crystalline phase. These can be solution-reprecipitation, topotactic nucleation and growth or some other mechanism. Several seeding experiments were conducted to elucidate the mechanism involved. It is found that the addition of previously crystallized seed material to the amorphous powder prior to the hydrothermal treatment doesn't significantly changes the particle size distribution. Taking into consideration all the observations it is inferred that the mechanism of hydrothermal crystallization under experimental conditions is predominantly topotactic nucleation and growth.

List of figures

Figure 1.2.1.	Crystallization mechanism in acidic pH range.....	8
Figure 1.4.1.	Mechanism of the formation of interparticle bonds leading to the formation of hard agglomerates.....	17
Figure 1.4.2.	Structure of hydrated zirconium oxide.....	18
Figure 1.4.3.	Mechanism of the formation of unagglomerated particles in presence of alcohol.....	18
Figure 2.1.1.	Schematic of the experimental procedure.....	22
Figure 2.1.2.	Schematic of the setup used for urea hydrolysis.....	24
Figure 2.1.3.	Schematic diagram of the furnace setup.....	29
Figure 2.2.1.	Angular separation of $K\alpha$ doublet as a function of 2θ	38
Figure 2.2.2.	Curves for correcting line breadths for $K\alpha$ doublet broadening.....	39
Figure 2.2.3.	Corrected full width half maximum for silicon as a function of diffraction angle.....	39
Figure 2.2.4.	Curves for correcting x-ray diffractometer line breadths for instrumental broadening under conditions of high resolution.....	40
Figure 3.1.1	Time for precipitation in urea hydrolysis of 0.5m/l ZrO_2 -10 mole % gadolinia containing different amounts of urea.....	44
Figure 3.1.2.	Variation of pH with time during urea hydrolysis.....	46

Figure 3.1.3.	X-ray diffraction plots for the hydrolysis product under different conditions of drying and washing	48
Figure 3.1.4.	Electron probe microanalysis of the dried powder obtained after urea hydrolysis.....	49
Figure 3.1.5.	X-ray diffractograms of powders sampled out after different periods of urea hydrolysis as mentioned in the figure.....	50
Figure 3.1.6.	Limiting particle size distributions of the amorphous powder.....	51
Figure 3.1.7.	The X-Ray Diffractogram of the Amorphous Powder.....	52
Figure 3.1.8.	Thermo gravimetric analysis of (a) amorphous powder and (b) crystalline powder.....	52
Figure 3.1.9	FTIR spectrum of the amorphous and crystalline powder hydrothermally crystallized at 320 ^o C, ~2 Mpa for 6 hours.....	53
Figure 3.2.1	X-Ray diffractograms from powders hydrothermally crystallized at different temperatures and pressures as mentioned in the figure.....	54
Figure 3.2.2	Particle size distribution of the (a) amorphous gel powder and the crystalline powders obtained from it by hydrothermal treatment at (b)220 ^o C, 1.6 MPa, (c) 260 ^o C, 1.8 MPa, (d) 300 ^o C, 2.0 MPa, and (e) 320 ^o C, 2.0 MPa.....	58
Figure 3.2.3	SEM image of the powders hydrothermally crystallized at 220 ^o C, 1.6 MPa for 6 hours.....	59
Figure 3.2.4.	Particle size distribution of the (a) amorphous powder and the powders hydrothermally crystallized from it at 320 ^o C, 2MPq for 6 hours at (b) pH 3, (c) pH 5, (d) pH 9, (e) pH 11.....	61

Figure 3.2.5.	X-ray diffractograms of zirconia powders hydrothermally crystallized at 270°C, ~1.8 MPa for 6 hours with different amount of gadolinia.....	62
Figure 3.2.6.	X-ray diffractograms from the powders hydrothermally crystallized at 220°C for 6 hours at pressures (a) 1.3 MPa, (b) 1.6 MPa, (c) 2.1 MPa...	63
Figure 3.2.7.	X-ray diffractograms of the powders after hydrothermal crystallization at a temperature of 220°C, 2 MPa pressure for 2 hours with steam to water ratio of (a) 3:1, (b) 1:1, (c) 1:3.....	64
Figure 3.2.8	Particle size distribution of the powders seeded with different amount of crystalline material and hydrothermally crystallized at 320°C, 2MPa for 6 hours. The particle size distribution of the (a) amorphous powder and the (b).crystalline seed is given for comparison. (c) 0.5 % seeded, (d) 5 % seeded, (e) 50 % seeded.....	66
Figure 3.2.9.	Particle size distribution of the powders seeded with different amount of crystalline material and hydrothermally crystallized at 320°C, 2MPa for 6 hours. The particle size distribution of the (a) amorphous powder and the (b) crystalline seed is given for comparison. (c) 0.5 % seeded, (d) 50 % seeded.....	67
Figure 3.2.10.	X-ray diffractograms of the powders hydrothermally crystallized with 5% seed material (prepared by hydrothermal crystallization at 320°C, 2MPa for 6 hours) for 6 hours at temperatures indicated in the figure.....	68
Figure 3.2.11.	Particle size distribution of the amorphous powder and the powder hydrothermally crystallized form it at 320°C, 2 MPa for 6 hours: the starting particle sizes are different.....	70

Figure 3.2 12. Particle size distribution of the powders hydrothermally crystallized at 320°C, 2 MPa for 6 hours with 10 minutes ultrasonication before hydrothermal treatment. Powders hydrothermally crystallized under similar conditions without ultrasonication is also shown for comparison.⁷¹

List of tables

Table 1.1.1	Comparison between different chemical routes for ceramic powder preparation...	2
Table 1.1.2.	Different hydrothermal synthesis routes.....	3
Table 1.2.1.	Phases present and crystallite size of hydrothermal products for different mineralizers.....	11
Table 2.1.1.	Conditions of hydrothermal crystallization.....	28
Table 2.1.3.	Workable pressure for the tubes with different diameter and thickness...	30
Table 2.1.4.	Properties of superheated steam.....	31
Table 2.2.1.	Hydrothermal crystallization under different conditions.....	33
Table 2.2.2.	Different instruments used for characterization.....	34
Table 3.1.1.	Time for precipitation in urea hydrolysis of 0.5m/L ZrO ₂ -10 mole % gadolinia containing different amounts of urea.....	43
Table 3.1.2.	Effect of different gadolinia content on the urea hydrolysis.....	45
Table 3.2.1.	Conditions of the preparation of amorphous powder used in hydrothermal crystallization.....	55
Table 3.2.2	The Effect of the hydrothermal treatment condition on the crystallite size	56

Hydrothermal Preparation of Ultrafine Powders

1.1 INTRODUCTION

In recent times there has been great emphasis on the ultra fine powders. Such powders can be sintered at much lower temperature and dense polycrystalline materials with very fine grain size can be obtained. In general chemical methods are employed in the preparation of powders to achieve the requirements of ultra fine particle size and compositional homogeneity. Of the different chemical routes – sol gel, co precipitation, hydrothermal etc, the hydrothermal route gives a better control over the particle size distribution and homogeneity. A comparison of hydrothermal technique with other preparatory routes has been given in table 1.1.1 ¹.

Hydrothermal synthesis involves the use of superheated steam (or pressurized hot water) for the preparation of crystalline anhydrous ceramic powder. The major differences between hydrothermal processing and other technologies is that there is no need for high temperature calcinations. Thus in turn the need of milling is eliminated. Powders can be

Table 1.1.1. Comparison between different chemical routes for ceramic powder preparation ¹

	Conventional	Sol-gel	Coprecipitation	Hydrothermal
Cost	Low/medium	High	Medium	Medium
State of development	Commercial	R & D	Commercial/ Demonstration	Commercial/ Demonstration
Compositional control	Poor	Excellent	Good	Good/excellent
Morphology control	Poor	Moderate	Moderate	Good
Reactivity	Poor	Moderate	Moderate	Good
Purity	<99.5 %	>99.5 %	>99.5 %	>99.5 %
Calcination	Yes	Yes	Yes	No
Milling	Yes	Yes	Yes	No

formed directly from solutions by complex reactions that take place in high temperature water. By controlling these reactions, it is possible to produce anhydrous crystalline powders with controlled particle size, controlled stoichiometry and in some cases controlled particle shape too. Advantages of this process also include the use of relatively inexpensive raw materials and elimination of impurities and structural defects associated with milling.

The use of hot pressurized water for the precipitation of oxides has been known for decades. Initially the hydrothermal literature was based very largely on the geosciences concentrating on simulating conditions that exist inside the earth to produce synthetic minerals. Naturally minerals are supposed to crystallize from the magma

beneath the earth crust under high pressure-temperature conditions prevailing there in presence of different mineralizers that boost the process.

It was Moorey² who did the first comprehensive study of the hydrothermal synthesis in ceramics. He investigated the underlying theory of hydrothermal synthesis using silica-water as the model. The solubility of silica was found to increase in supercritical water and solution reprecipitation was proposed as the mechanism of hydrothermal synthesis. Since then hydrothermal synthesis has developed a lot and now hydrothermal technique has been exploited in different ways to produce ceramic powders. A complete list has been given in table 1.1.2³.

Table 1.1.2. Different hydrothermal synthesis routes ³

Hydrothermal crystal growth
Hydrothermal treatment
Hydrothermal alteration
Hydrothermal dehydration
Hydrothermal extraction
Hydrothermal reaction sintering
Hydrothermal sintering corrosion reaction
Hydrothermal oxidation
Hydrothermal precipitation
Hydrothermal crystallization
Hydrothermal decomposition
Hydrothermal hydrolysis + Hydrothermal precipitation
Hydrothermal electrochemical reaction
Hydrothermal mechano-chemical reaction
Hydrothermal + ultrasonic
Hydrothermal + microwave

Zirconia ceramics are one of the most active areas of research today because of their excellent mechanical properties coupled with high oxygen ion conductivity and thermal properties. The high oxygen conductivity makes them suitable for sensors and as electrolytes in solid oxygen fuel cells. Zirconia exists in three polymorphic forms – monoclinic, tetragonal and cubic. Orthorhombic and hexagonal forms of zirconia can be also synthesized under special conditions. Though monoclinic is the thermodynamically most stable phase in pure form at room temperature, it is the cubic phase that has the highest conductivity followed by the tetragonal phase. The high temperature cubic phase can be stabilized at room temperature by doping zirconia with several divalent and trivalent oxides, the notables being Y_2O_3 , Gd_2O_3 , CaO and MgO .

Hydrothermal technique provides a suitable route for the preparation of tetragonal as well as cubic zirconia at temperatures just a little above $100^\circ\text{C}^{4,7}$. The different methods that can be used for the preparation of fine zirconia powder are

Hydrothermal oxidation

Hydrothermal decomposition

Hydrothermal homogeneous decomposition

Hydrothermal crystallization

The reactive electrode submerged process

Of these the hydrothermal crystallization is an interesting method of producing nanocrystalline zirconia powder. In general the process can be described as follows. An amorphous powder, generally precipitated from its salt solution by changing the pH, taking advantage of the pH dependence of solubility, is suspended in water or salt solution and subjected to supercritical temperature, pressure of water for different durations ranging from few hours to few days. On cooling a fine powder is obtained. The salt ions are supposed to act as mineralizers.

1.2 MECHANISM OF HYDROTHERMAL CRYSTALLIZATION

The effects of pH and different mineralizers have been well studied. On the basis of these studies three mechanisms have been proposed.

⇒ The solution reprecipitation mechanism in which the metastable, intermediate stable or amorphous phase dissolves in the suspending medium under supercritical conditions of water and the stable phase crystallizes from the solution.

⇒ The formation of crystallites of metastable phases of zirconia from the amorphous powder with a gross morphology resembling the amorphous powder followed by their spontaneous coalescence to form stable crystalline phase.

⇒ The topotactic crystallization, in which the short range, ordered regions in the amorphous material act as nucleation sites for the crystallization of the stable phase.

1.2.1 HYDROTHERMAL CRYSTALLIZATION AT ACIDIC pH

In a significant study, Adair et al.⁸ studied the effect of pH on the hydrothermal crystallization. Hydrothermal treatments of 0.2 M zirconium oxynitrate were done at different temperatures (110°C, 175°C, 200°C) and times at different pH (0.5, 3.6, 12.1) the pH value being adjusted by the addition of 5M KOH. The crystallization under these conditions is characterized by an initial induction period followed by rapid crystallization at a more or less constant rate and then by decreasing rate of crystallization. At lower pH values only monoclinic (m) phase has been found to crystallize whatever might be the temperature and duration of hydrothermal treatment. However at intermediate pH, the m phase crystallizes at lower temperatures whereas at higher temperatures both tetragonal and monoclinic phases form. Also higher the temperature and pH, lesser is the time required for complete crystallization. Another important factor is that though potential

stabilizers like K^+ ions were present, cubic zirconia was never obtained during the study. The formation of m-ZrO₂ was proposed to be by the first mechanism. The X-ray amorphous precursor undergoes transient dissolution to form hydrated species which recrystallize to form m-ZrO₂. A schematic diagram for the mechanism is given in fig 1.2.1.

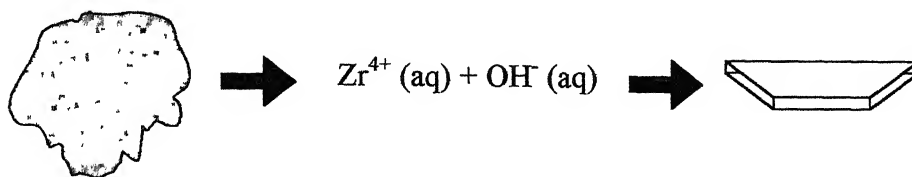


Figure 1.2.1. Crystallization mechanism in acidic pH range

Another study by the same authors ⁹ confirms the same classical precipitation process operating during the hydrothermal crystallization. They produced equiaxed, nonagglomerated m-ZrO₂ from homogeneous solutions at lower pH and high supersaturations. Also it was shown that higher the supersaturation lower the particle size which suggests the classical nucleation-growth process from solution.

It is well known that upon dissolution, the zirconyl salts liberate ZrO^{2+} which combines with water rapidly forming hydroxylated sites and finally forms soluble tetramers of $[Zr(OH)_2 \cdot 4H_2O]_4^{8+}$. These tetramers have a square, planar, array of zirconium atoms. These tetramers when subjected to heat and certain other conditions form their own dimers and other higher order assemblies. Nucleation from these aggregates is favorable when the aggregation number approaches 12 to 24.

In a similar study involving direct crystallization of m-ZrO₂ from zirconyl salts, Cannon and Bleier⁵ reported hydrothermal crystallization by the first and the second mechanisms. Metastable zirconia has been reported to form in the acidic pH range by the polymerization of $[Zr(OH)_2 \cdot 4H_2O]_4^{8+}$ tetramers or their two dimensional networks via

condensation of water molecules between hydroxylated bonds. The product was shown to have cubic symmetry. The cubic quasicrystals orient themselves to form m-ZrO₂ primary particles of the order of 3 nm

This mechanism is supported in a recent study by Cheng et al¹⁰. Zirconium oxychloride octahydrate was used as the starting material. KOH was used to adjust the pH. Hydrothermal treatment was done at 220°C for 2 hours. However monoclinic crystals were proposed to form directly by the condensation of $[\text{Zr}(\text{OH})_2 \cdot 4\text{H}_2\text{O}]_4^{8+}$ tetramers which further aggregate to form spindle agglomerates. This contradicts the results of Cannon and Bleier⁵ who proposed the formation of cubic quasicrystals as the intermediate step between amorphous and the final monoclinic crystallites.

1.2.2 HYDROTHERMAL CRYSTALLIZATION AT BASIC pH

Though there is little dispute about the mechanism of hydrothermal crystallization at lower pH, different opinions regarding the crystallization mechanisms and metastable phase at higher pH have been found in the literature.

In one of the earlier studies, Nashizawa et al¹¹ reported the crystallization of dried amorphous powder obtained by the ammonia hydrolysis of zirconium oxychloride at as low as 130°C when 4 molal NaOH was used as mineralizer. However, at lower concentration of sodium hydroxide the crystallization occurs at higher temperatures. EPMA indicated that Na⁺ is introduced during crystallization. The metastable and the final phases are found to vary with NaOH concentration. When the concentration of sodium hydroxide was ≤ 0.7 molal, tetragonal zirconia appears together with the monoclinic phase in the initial stages of crystallization and both form remain up to 350°C, the maximum temperature applied in the investigation. Similar behavior was observed for

the hydrothermal crystallization of zirconia when water is used as mineralizer, the amorphous powder being crystallized at 265°C forming monoclinic and tetragonal zirconia in the ratio 40:60 which remains unchanged on further hydrothermal treatment. Upon increasing the NaOH concentration the tetragonal crystallite size increases slightly up to 25nm, though the amount decreases and becomes zero for NaOH concentrations ≥ 1 molal. In NaOH solutions ≥ 1 molal, cubic zirconia crystallizes initially and abruptly transforms to needle like monoclinic crystallites. Study of XRD spot patterns revealed cubic crystallites arranged in highly oriented manner in a powder prepared at 260°C. However at higher temperatures the monoclinic single crystals were found to be surrounded by very fine cubic crystallites. From the decrease of cubic crystallite size with NaOH concentration it was proposed that Na^+ (and OH^-) adsorbed on the amorphous powder rupture the $\text{Zr} - \text{O} - \text{Zr}$ bonds, collapsing the structure leading to the formation of cubic crystallites with slight rearrangement. These very fine crystallites were supposed to behave like colloidal particles. The formation of needle shaped crystals was speculated to be due to the migration and alignment of these cubic crystallites in highly ordered fashion. Also the Na^+ incorporated into the structure was excluded during the transformation. However no evidence was presented and also the formation mechanism at $\text{pH} \leq 1$ was not dealt with.

Mirowslaw et al¹²⁻¹⁴ also supported the coalescence mechanism. ZrO_2 , $\text{ZrO}_2\text{-Y}_2\text{O}_3$, $\text{ZrO}_2\text{-CaO}$ systems were studied. Ammonia hydrolyzed gel coprecipitated from their zirconyl chloride and other related chlorides were used as starting material. The different mineralizers used were NaOH, LiOH, KOH, NaCl, KCl, LiCl separately or in mixtures and water. Hydrothermal treatment was done at 250°C for different durations. While in basic medium, elongated monoclinic crystals were obtained; smaller isometric crystals

were obtained when water was used. Also the particle size distribution of the powder was bimodal or trimodal when prepared in basic medium but unimodal distribution has been obtained when prepared in water. Fixed ratios of larger to smaller particles prove the coalescence theory. The fact was consistent with a TEM micrograph that shows a monoclinic crystal composed of two smaller crystallites. However the diffraction pattern was typical for the single crystal proving high crystallographic orientation within the crystal assembly. From the unimodal distribution of the powder prepared in water it seems a separate mechanism is being operative in water.

However in a detailed investigation¹³ later it was shown that same mechanism has been operating in both the cases; only too slowly in the case of water. Hydrothermal treatment of the same ammonia hydrolyzed powder was done with 4moles/liter NaOH and H₂O as mineralizers at 250°C for different times. After one hour of hydrothermal treatment two different sizes of particles were observed. On the basis of X-ray line broadening it has been found that the smaller crystallites had tetragonal symmetry and bigger ones were of monoclinic symmetry. With time well-defined necks occurred between the bigger particles. The formation of necks was attributed to the dissolution precipitation mechanism; materials from the convex surface dissolved to precipitate on the concave surfaces. The prolonged hydrothermal treatment causes the disappearances of the smaller particles and finally after 90 minutes, lathe shaped monoclinic particles appear. In water the same mechanism was found to occur but only too slowly. Particles shapes are same in both the cases but the sizes were different especially of the monoclinic phase. The rearrangement of the crystallites in a highly oriented manner was attributed to the zero dihedral angle in water- oxide systems resulting in low energy contacts between

zirconia particles. So the mechanism of hydrothermal crystallization was proposed to be a two-step process.

1. Coalescence of the individual crystallites in highly oriented manner
2. Increase of contact by the dissolution-precipitation process leading to the smoothening of the elongated particle faces and smaller isometric crystallites.

The mechanism of formation of the tiny crystallites in the initial stages was not investigated

However for ZrO_2 - Y_2O_3 system elongated monoclinic crystallites were formed for lower Y_2O_3 content together with smaller isometric tetragonal/cubic crystallites whose content increases with Y_2O_3 content. This might be due to the decrease in solubility of the amorphous powder in the hydrothermal medium leading to the crystallization by topotactic means as pointed out by Yoshimura¹⁶ and discussed later in this chapter. To study the effect of Na^+ ions in the formation of crystallites as pointed out by Nashijawa¹¹ hydrothermal treatment was done with NaCl. Small isometric crystals (of the order of 9.5 nm) of cubic or tetragonal symmetry were observed to form but the coalescence of those isometric crystals were not observed. It seems that either the OH^- ions plays an important role during the coalescence or Cl^- ions adversely affect the process or both. Studies on ZrO_2 - CaO system show similar trend. In a NaOH rich solution the elongated crystals are found to grow very fast compared to solutions without surplus NaOH. However, change in NaOH concentration didn't seem to affect the process very much.

In yet another investigation¹⁴ by the same author about the phase composition it was shown that small isometric tetragonal crystallites transform with time into small isometric monoclinic particles and the latter convert to the elongated crystallites with no phase change. The formation of zirconia by solution reprecipitation was ruled out because

addition of amorphous gel to isometric crystallites prepared under the same conditions followed by hydrothermal treatment doesn't hasten up the growth process.

Yoshimura et al¹⁵⁻¹⁷ presented a different theory about the hydrothermal crystallization. They proposed that both dissolution-precipitation and topotactic crystallization are operative during hydrothermal crystallization depending on the solubility of the amorphous material in the suspending medium under supercritical condition. The starting material was amorphous hydrated zirconia precipitated from Hf free $ZrCl_4$ solution with NH_4OH , then washed with distilled water and dried at $120^\circ C$ for 48 hours. The different mineralizers and the corresponding phases and their crystallite sizes after hydrothermal treatment at $300^\circ C$, 100 MPa for 24 hours is tabulated in table 1.2.1¹⁶.

Table 1.2.1. Phases present and crystallite size of hydrothermal products for different mineralizers¹⁶

Mineralizer	Average crystallite size of products (nm)	
	t- ZrO_2	m- ZrO_2
KF (8 wt. %)	Not detected	16 nm
NaOH (30 wt. %)	Not detected	40 nm
H_2O	15 nm	17 nm
LiCl	15 nm	19 nm
KBr	13 nm	15 nm

Also hydrothermal treatment at different temperatures ranging from $200^\circ C$ to $600^\circ C$ was done. LiCl concentration was varied up to 30 wt. % to study the effect of mineralizer concentration. Amorphous powders calcined at different temperatures ($240^\circ C$, $420^\circ C$, $620^\circ C$, and $820^\circ C$ in air for 60 minutes) were also used as starting material. XRD showed that samples calcined below $240^\circ C$ contained only amorphous phase; at $420^\circ C$ both

tetragonal and monoclinic phases formed, whereas only monoclinic phase was present at 820°C. The phases produced by the hydrothermal treatment of these phases were completely different. Samples calcined at 240°C produced tetragonal and monoclinic phases on hydrothermal treatment. However hydrothermal treatment of the samples calcined at 420°C produced monoclinic phase only. Tetragonal zirconia was found to crystallize from amorphous zirconia only. Both tetragonal and monoclinic zirconia was formed when H₂O, LiCl, KBr solutions were used, whereas only monoclinic zirconia was produced with KF and NaOH solution. Use of 8 weight percent KF and hydrothermal treatment at 100 MPa for 24 hours at different temperatures from 200°C to 600°C produced some interesting results. Crystallite size of monoclinic zirconia produced was ≈16nm at 200°C, and increased gradually up to ≈22 nm at 500°C. Abrupt increase in crystallite size was observed on further increasing the hydrothermal temperature, 70 nm at 550°C and > 100 nm at 600°C. In NaOH solution, the crystallite size growth was even larger. From these results the formation of monoclinic zirconia was proposed to be via solution reprecipitation. These results are consistent with the fact that solubility of zirconia increases rapidly in KF solution with temperature. However as tetragonal zirconia was formed from amorphous powder only when the solubility of zirconia in the mineralizers is low as in the case of H₂O, LiCl, and KBr solution, it was proposed that tetragonal zirconia was forming by topotactic crystallization. Study of the distribution functions obtained from X-ray and neutron diffraction by Livage et al¹⁸ showed that atoms in amorphous zirconia are not distributed at random completely, rather certain preferred interatomic spacings corresponding to tetragonal zirconia exist in short range ordered regions. These might be acting as the nucleation sites for topotactic crystallization.

Adair et al⁸ proposed that with significant concentration of hydroxyl ions at higher pH, the gel chemistry must be playing an important role in the crystallization from amorphous powder under hydrothermal conditions. The higher pH derived gel was proposed to possess a higher energy state and, therefore a lower activation barrier for crystallization. The hypothesis was supported by calculating the activation energies at different pH regions from the crystallization rates assuming Arrhenius type reaction.

So though dissolution reprecipitation seems to be the mechanism of hydrothermal crystallization at low pH, there is much dispute about the hydrothermal crystallization mechanism at higher pH values.

The different mechanisms proposed are

- Coalescence Mechanism¹¹

- Coalescence + Dissolution-Reprecipitation¹²⁻¹⁴

- Topotactic Crystallization and Dissolution-Reprecipitation depending on the solubility¹⁵⁻¹⁷

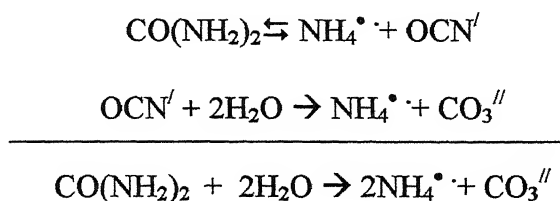
- Nucleation and Growth from the high-energy low-density amorphous gel.

1.3 UREA HYDROLYSIS

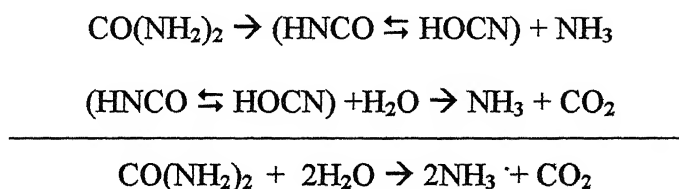
Ammonia hydrolysis provides an easy way to produce amorphous hydrous zirconia powder, which can be hydrothermally crystallized to get the various crystalline zirconia phases. But urea hydrolysis is a better technique because ammonia is released in this process in a very controlled way as discussed later. This produces a finer powder than that produced in ammonia hydrolysis.

The mechanism of urea hydrolysis has been studied long ago. It has been proposed that the hydrolysis of urea is a two-step process rather than direct decomposition into ammonia and carbondioxide.¹⁹⁻²³ Urea first decomposes into cyanic

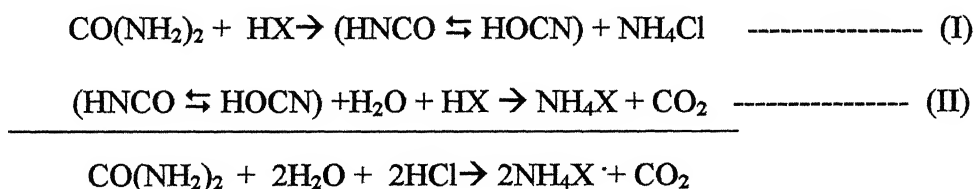
acid (or cyanate ions) and ammonia (or ammonium ions) at $\sim 100^\circ\text{C}$. In the second stage the cyanic acid (or cyanate ions) reacts with water and decomposes into ammonia (or ammonium ions) and carbondioxide (or carbonate ions). The second step is irreversible. The reaction is illustrated in ionic form by the following reactions¹⁹.



The mechanism has been illustrated in compound form also^{20,21}.

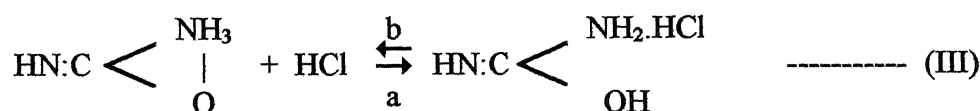


However in presence of acids the decomposition reaction of urea has been found to be slightly different.^{21,22}



Apart from the decomposition, urea (having a pronounced basic nature) also forms urea salt with the acid e.g. urea chloride in presence of hydrochloric acid. However this reaction is only partial. In a normal solution of urea and hydrochloric acid only $\sim 45\%$ of the urea remains undissociated as urea hydrochloride.²²

The reaction can be illustrated as follows

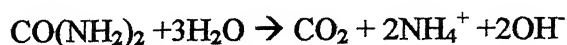


Since it is the free urea that decomposes the rate of decomposition at any point of time will surely be controlled by the amount of free urea present. The hydrolysis of cyanic acid, being a very fast reaction, results in removal of the intermediate products as fast as they are produced. The equilibrium of the reaction (II) is shifted to the right. Following the La Chatelier's principle this will result in the faster decomposition of urea into cyanic acid and ammonia by the reaction (I). So though urea is fixed as a salt at the onset (reaction (III) in the direction 'a') decomposes rapidly (reaction (III) in the direction 'b') to continue the reaction (I).

It has been observed that weaker the acid faster the dissociation of urea²¹. This has been attributed to the presence of more free urea in presence of weak acid as less urea is fixed as urea salt at the beginning.

In a later study²³ the same fact was confirmed. Also it was shown that with sulphuric acid the urea hydrolysis is twice as fast as in the aqueous solution.

H. Y. Xiang et al²⁴ produced nanosized monoclinic particles by urea hydrolysis for extended time of about 50 hours. Zirconyl chloride octahydrate was used as starting material. It is well known that Zr^{4+} ions are present as $[Zr_4(OH)_8 \cdot 16H_2O]^{8+}$ tetramers in aqueous solution. It was proposed that during urea hydrolysis the four-coordinated water molecules were replaced by hydroxyl ions obtained from the decomposition of urea according to the following reaction, which is a slight variation of the reactions mentioned before in this chapter.



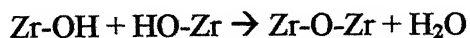
Condensation between the hydroxyl ions coordinated groups produce 'fluffy' crystal nuclei, which grows with boiling time to form the least symmetric zirconia phase i.e. the monoclinic phase. The agglomeration of the hydrolysis products was proposed to depend

on the pH of the solution ie amount of OH⁻ present. Higher the pH faster is the agglomeration.

1.4. ROLE OF WASHING IN THE PREPARATION OF FINE POWDER

Washing is also a significant step in the preparation of unagglomerated powders. It removes the undesired products like chlorine, ammonia etc that remain adhered to the particles and affect the properties of the product. Chlorine is known to hinder the sintering and densification of zirconia powders but enhances particle coarsening by Oswald ripening.²⁵ For the removal of chlorine the usual practice is repeated washing with warm water until there is no trace of chlorine in the wash effluent. Drying of water washed powders leads to the formation of hard agglomerates. These agglomerates do not break during compaction, which results in incomplete densification. To prepare unagglomerated powder water is replaced by some organic liquids (usually some alcohol or acetone) in the final washing step. Freeze drying²⁶ and azeotropic distillation²⁷ are the other techniques that have been successfully used to prepare unagglomerated powder. The role of alcohol for obtaining unagglomerated powders has been extensively investigated.²⁸⁻³⁰

Powders washed with water have chemically adsorbed hydroxyl ions and water molecules on their surface. During drying the surface adsorbed species on the neighboring particles undergo condensation reaction and interparticle Zr-O-Zr bonds are formed. This leads to formation of hard agglomerates



The mechanism is illustrated in figure 1.2. During drying the encircled water molecules vaporizes forming Zr-O-Zr bonds.

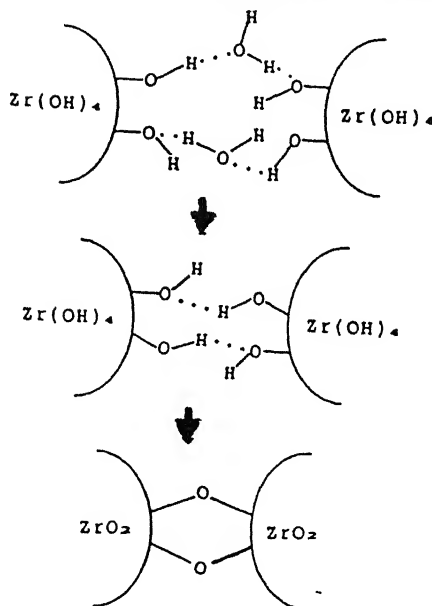


Figure 1.4.1. Mechanism of the formation of interparticle bonds leading to the formation of hard agglomerates.

Norman and Jones²⁸ showed that methanol is capable of removing the nonbridging hydroxyl groups and coordinated water thereby hindering the condensation reaction. However whether methanol is adsorbed on the surface of the particles instead of the water or hydroxyl ions was not mentioned. Ready et al²⁹ proposed that the alcohol molecules form hydroxyl bonds with the surface adsorbed hydroxyl ions. This inhibits interparticle hydrogen bonding. Also due to their bulky size the alcohol molecules cause steric hindrance not allowing the particles to come in close proximity. Later the mechanism was further elucidated.³⁰ Based on the structure of hydrated zirconium oxide by Zaitsev³¹ (shown in fig 1.4.2) Kaliszewski and Heuer³⁰ showed ethanol molecules are directly attached to the surface of the hydrated zirconium tetramers rather than forming hydrogen bonds with the surface adsorbed hydroxyl ions using FTIR. However the replacement of hydroxyl ions was only partial but that was effective enough to produce unagglomerated powder. During drying the oxy groups (ethoxy if ethanol is used, methoxy if methanol is used or propoxy for propanol) reacts with each other forming

corresponding alkenes or ethers (e.g. ethylene for ethanol, propylene for propanol or dimethyl ether for methanol) and water. Also it was postulated that removal of the ethoxy groups occurs preferentially between neighboring groups of same particle as close approach of particle are inhibited due to steric hindrance. The mechanism is illustrated in the fig 1.4.3.

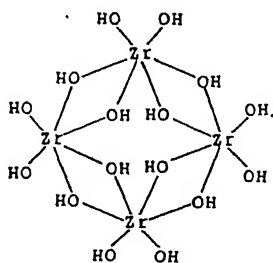


Figure 1.4.2. Structure of hydrated zirconium oxide³¹

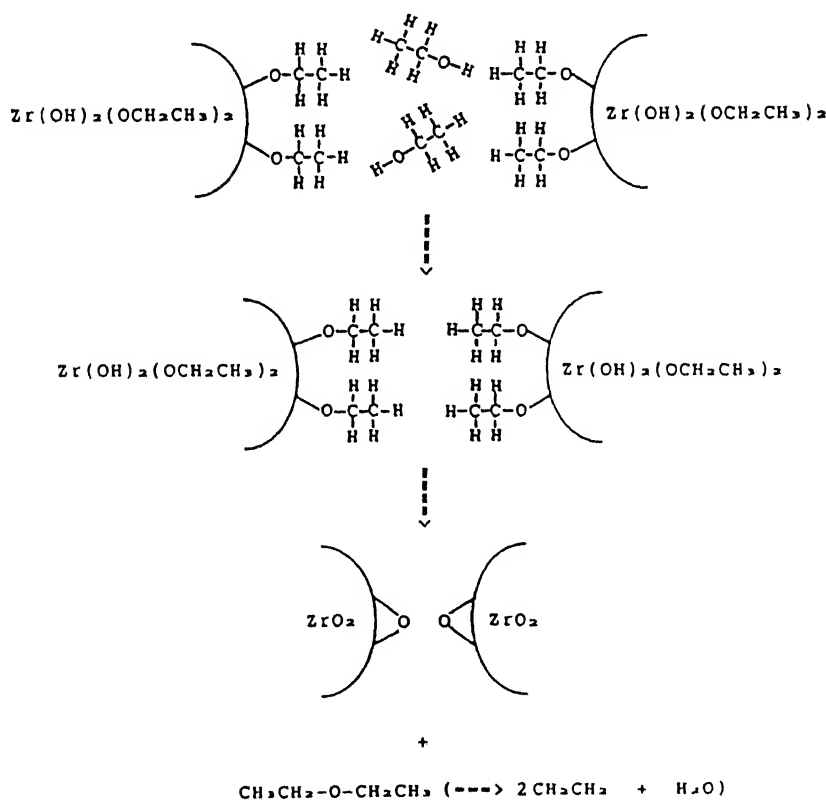


Figure 1.4.3. Mechanism of the formation of unagglomerated particles in presence of alcohol²⁷

Recently gadolinia doped zirconia has gained much interest. Its ionic conductivity is supposed to be higher than most of stabilized zirconia systems because of its small size difference with zirconium ions.³¹ However, there is much contradiction about the ionic conductivity in the literature. So gadolinia doped zirconia was chosen for the study of hydrothermal crystallization. 10% gadolinia doped zirconia has been found to produce pure cubic zirconia, the zirconia phase with highest conductivity.

1.5. STATEMENT OF THE PROBLEM

As is evident from the above discussion, the formation of the various crystalline phases of zirconia by hydrothermal precipitation or hydrothermal crystallization is still not clearly understood.

Nanocrystalline powders of ceramics in general and zirconia in particular are of great scientific and technical interest. Methods such as sol-gel, coprecipitation etc are capable of yielding nanosized powders but these powders are amorphous and the high temperature calcinations required to crystallize them also results in their coarsening. The hydrothermal technique on the other hand can directly yield crystalline nanopowders.

For technical applications (such as solid electrolyte, structural applications) stabilized zirconia are used. The most well known stabilizers are MgO, CaO, Y₂O₃, and Ce₂O₃. The oxide Gd₂O₃ is also known to stabilize zirconia, but preparation of Gd₂O₃ doped ZrO₂ powders is difficult. It is of interest to study Gd₂O₃-ZrO₂ ceramics because of such properties as higher electrical conductivity etc.

Based on the above, the present work has been aimed at the following:

1. To investigate if it is possible to prepare Gd_2O_3 - stabilized zirconia powders of different compositions by hydrothermal crystallization.
2. To determine the condition for the condition for the preparation of nanosized ZrO_2 - Gd_2O_3 powders.
3. To carry out experiments to understand the mechanism of the hydrothermal crystallization in ZrO_2 - Gd_2O_3 alloys

The experiments carried out and the experimental techniques adopted are described in the next chapter (Chapter 2). The results are presented and discussed in chapter 3. Finally the conclusions are presented in the last chapter (Chapter 4).

2 Experimental Procedure

2.1 POWDER PREPARATION

Zirconia powders stabilized with gadolinia was prepared in two steps

1. Preparation of dried zirconia gel by urea hydrolysis followed by the removal of chlorine, dewatering by n-propanol and drying at 80°C.
2. Hydrothermal crystallization of the dried zirconia gel to produce fine crystalline powders.

The schematic of the experimental procedure is given in fig 2.1.1.

Though ammonia hydrolysis provides an easier route for the preparation of amorphous zirconia, urea hydrolysis provides a better control over the hydrolysis reaction. Ammonia is released in two steps and it is easier to control the hydrolysis reaction by varying the urea concentration, time of reaction, and the temperature. Thus urea hydrolysis was favored over ammonia hydrolysis.

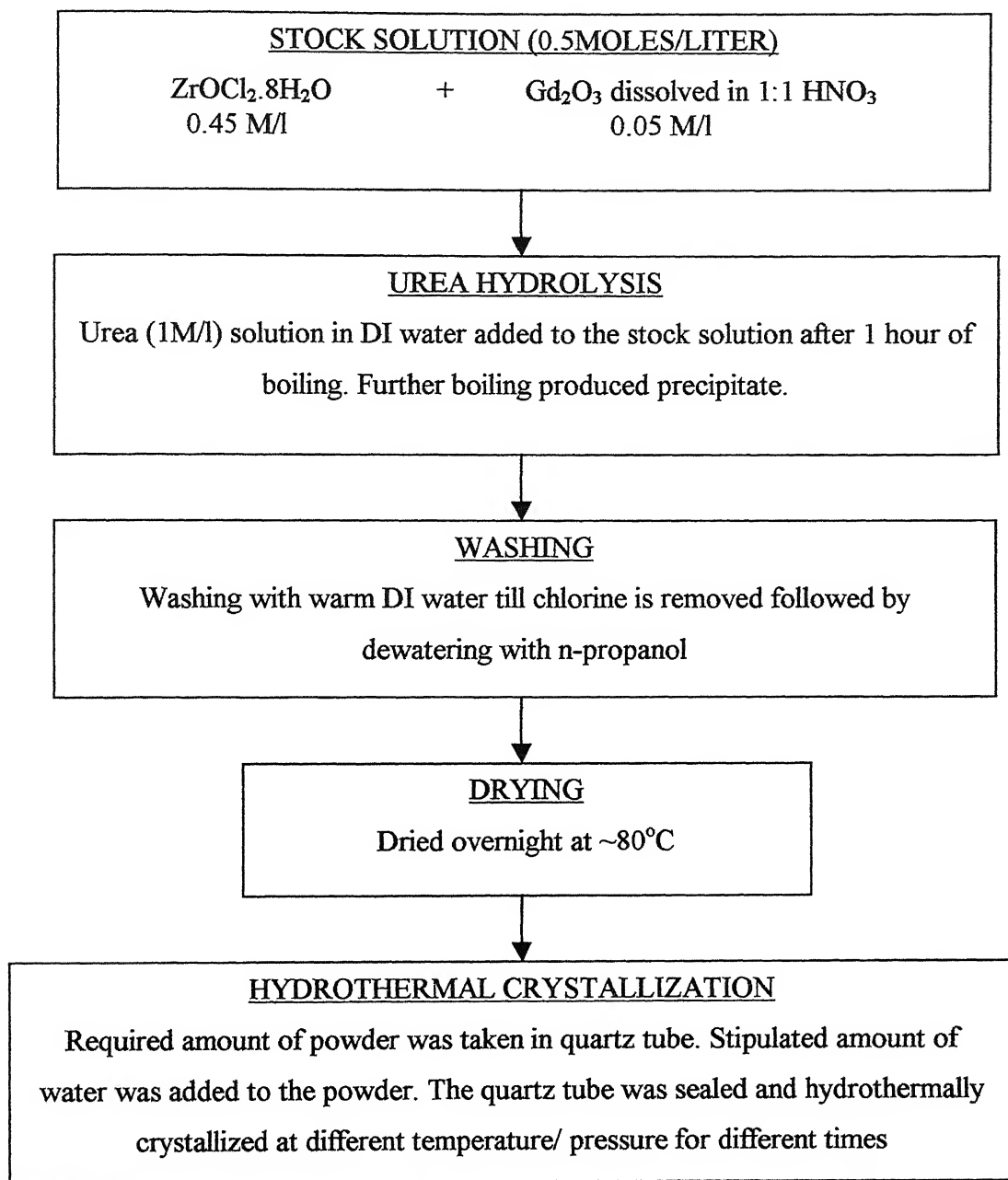


Figure 2.1.1. Schematic of the experimental procedure

The raw materials used for the preparation of stabilized zirconia are

Zirconyl chloride octahydrate (LR grade, Loba Chemie Pvt. Ltd. India)

Urea (AR grade, Thomas Becker Pvt. Ltd. India)

Gadolinium oxide (LR grade, Loba Chemie Pvt. Ltd. India)

Nitric acid (LR grade, Qualigen Fine Chemicals of Glaxo India Ltd.)

2.1.1. UREA HYDROLYSIS AND DRYING

Gadolinium oxide was dissolved in 1:1 nitric acid to form gadolinium nitrate. 100 ml of gadolinium nitrate and zirconyl chloride octahydrate (in the molar ratio $\text{ZrO}_2 : \text{Gd}_2\text{O}_3 :: 9:1$) solution was prepared by dissolving them in DI water (conductivity $<0.1\mu\text{S}$) followed by stirring for 30 minutes. The concentration of the solution was 0.5 moles/liter. Separately urea was also dissolved in DI water to form a 100 ml solution and stirred for 30 minutes. Urea was taken in excess (specific molecular ratio= 2) to ensure complete hydrolysis. Specific molecular ratio is defined as the ratio of number of moles of urea to the number of moles of metal salts.

In a typical run the amount of raw materials used are

Zirconyl chloride octahydrate $[\text{ZrOCl}_2 \cdot 8\text{H}_2\text{O}] \rightarrow 7.2507 \text{ gms}$

Gadolinia $[\text{Gd}_2\text{O}_3] \rightarrow 0.9063 \text{ gms}$

Urea $[\text{CO}(\text{NH}_2)_2] \rightarrow 3.003 \text{ gms}$

The zirconyl chloride, gadolinium nitrate solution was heated for 60 minutes at boiling ($\sim 105^\circ \text{C}$) prior to the addition of urea solution under constant stirring in three necked round-bottom flask fitted with a condenser and a thermometer. The round-bottom flask was put in oil bath to ensure constant temperature. A schematic diagram of the set up is shown in fig 2.1.2.

After another 150-180 minutes of heating the solution turns turbid and on further heating forms a milky white, thick jelly like precipitate. DI water was added to dilute it and stirring was continued till the pH rises to maximum. (~ 5). After that the heating was continued for another hour to ensure the completion of the reaction. Then the entire solution was quenched by putting the round-bottom flask in ice-cooled water. On standing under these conditions for a few hours, a thick precipitate was

obtained with clear supernatant mother liquor.

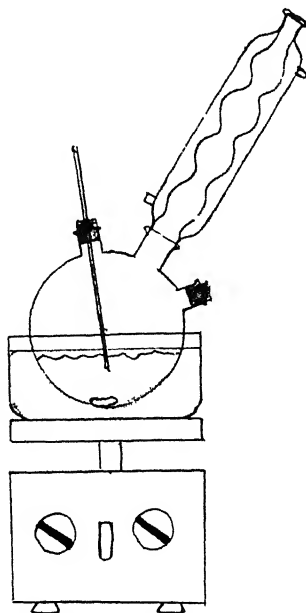


Figure 2.1.2. Schematic of the setup used for urea hydrolysis

After the urea hydrolysis the precipitate was separated from the mother liquor by centrifuging. The precipitate was washed repeatedly with luke warm water by stirring the precipitate in it for about 60 minutes and then centrifuging for about 30 minutes at ~ 5000 rpm. These steps are repeated until the wet gel was chlorine free. Each time the wash effluent was checked for chlorine by adding a few drops of N/50 silver nitrate solution to ~ 5 ml of the wash effluent. The centrifuging process was not sufficient to separate the ultrafine particles present in the precipitate. So the wash effluent was heated to $\sim 70^\circ\text{C}$ for some time. The ultrafine particles formed soft agglomerates due to the thermal energy. These agglomerates were separated from the wash liquid using a Whatmann 5 filter paper and the wash liquid was dried to estimate the amount of unreacted components and their phases. The filtered particles were washed with warm water on the filter paper itself until they were free of chlorine and then mixed with the bulk chlorine free precipitate. Then the chlorine free precipitate

was dewatered by adding n-propanol followed by stirring for 30 minutes and centrifuging at ~5000 rpm for another 30 minutes to remove the propanol. The propanol washed precipitate was suspended in fresh propanol after that and dried at room temperature for 5-6 hours followed by overnight oven drying at ~80°C. The dried powder formed soft agglomerates, which were broken with pestle mortar and then used for characterization and hydrothermal crystallization.

2.1.2 OPTIMIZATION OF UREA HYDROLYSIS

The urea hydrolysis process described above has been optimized in several steps as described below.

In the initial stages, urea hydrolysis was done in a slightly different way. Required amount of metal salts were dissolved in water to form 0.5moles/litre solution. Different amounts of urea (SMR = 0.5, 1, 1.8, 2, 3.6, 5.4, and 7.2) was added to the solution and heated for 6 hours at boiling (~105°C) in covered beakers. The time required for the precipitation of the mixed salts was noted. After 6 hours the powders were dry. It was not possible to separate the unreacted powder from the precipitate. So further urea hydrolysis trials were done under refluxing in a round bottom flask fitted with reflux condenser. Oil bath was used to ensure higher temperature. Bath temperature was maintained at 140°C. Water bath instead of oil bath was used in one trial. No precipitate was obtained because of lower temperature.

With SMR = 0.5 two trials were made. In one of them 1.5015 grams of urea was added in powder form to 100 ml of 0.5moles/litre $\text{ZrOCl}_2 \cdot 8\text{H}_2\text{O}$ - Gd_2O_3 solution while on the other same amount of urea was dissolved in 20 ml of DI water and same amount of metal salts were dissolved to form a 80 ml solution separately. Both the

solutions were mixed and heated at $\sim 105^{\circ}\text{C}$. In both cases the precipitate appeared after about 10 hours. So further urea hydrolysis were done with solution because of easier handling.

In the initial stages of urea hydrolysis in acid medium, urea is known to form urea salt with the acid (e.g. urea hydrochloride with hydrochloric acid) because of its basic nature. This reduces the overall rate of urea hydrolysis process, as it is the free urea that decomposes and reacts with the metal salts. To avoid this, the urea solution was first heated to 100°C for 2 hours and then the metal salt solution was added to it. But now there was no precipitate even after three hours of the addition of the metal salts. Precipitate was obtained only after further addition of urea. In another trial the salt solution was heated first to $\sim 100^{\circ}\text{C}$ and then urea solution was added to it. Precipitate was obtained after 3 hours of the addition of urea. Thus addition of urea to the hot salt solution seems to hasten the urea hydrolysis process.

In the above experiments Gd_2O_3 was used as the source of gadolinium. It was expected that the strong acidic environment of $\text{ZrOCl}_2 \cdot 8\text{H}_2\text{O}$ solution would be sufficient to dissolve the Gd_2O_3 . But the x-ray diffraction of the powder after urea hydrolysis showed the presence of Gd_2O_3 in the product. So instead of gadolinia, gadolinium nitrate and chloride was used for the urea hydrolysis. The wash effluent with the mother liquor was dried and heated at 900°C for 2 hours and characterized by x-ray diffraction to determine the phases.

The variation of pH with time during the urea hydrolysis process was observed after the process was optimized. Urea corresponding to $\text{SMR} = 2$ was dissolved in DI water to form a 100 ml solution. Similarly, metal salts were dissolved separately in DI water to form 100ml solution. The metal salt solution was heated for 1 hour at $\sim 100^{\circ}\text{C}$

for 1 hour before adding the urea solution. Small portions were pipette out at regular intervals, diluted 10 or 100 times with DI water and the pH was measured with a pH meter. The actual pH of the solution was calculated from the observed values as follows.

Suppose the actual pH is A. so the hydrogen ion concentration is 10^{-A} moles/litre When diluted by 10 times with DI water (pH ~ 7 i.e. $[H^+] = 10^{-7}$)

$$\begin{aligned}[H^+] &= \frac{1}{10} \times 10^{-A} + \frac{9}{10} \times 10^{-7} \\ &= 10^{-(A+1)} + (9 \times 10^{-8})\end{aligned}$$

Now when $A < 5$, the second term can be neglected.

So $[H^+] = 10^{-(A+1)}$; pH = $A+1 = P$ (say)

Therefore $A = P - 1$

Similarly, when diluted by 100 times $A = P - 2$

2.1.3. HYDROTHERMAL CRYSTALLIZATION

Hydrothermal crystallization was done in sealed quartz tubes. The gel powder and a calculated amount of water were put into a quartz tube. The quartz tube was sealed and then put in a wrought iron tube. The wrought iron tube with the sealed quartz tube inside was then kept at the center of the furnace muffle and held at the required temperature for 2 or 6 hours. No external pressure was used for the hydrothermal crystallization. The autogenous pressure of the superheated steam was sufficient for the hydrothermal crystallization. The pressure was varied by varying the amount of water initially added or the temperature. The different temperature, pressure, time for which hydrothermal crystallization was done is tabulated in table 2.1.1.

Table 2.1.1. Conditions of hydrothermal crystallization

Temperature (°C)	Pressure (MPa)	Time (hrs)	Condition of water
220	1.3	6	Superheated steam
	1.6	6	Superheated steam
	2.1	6	Superheated steam
	2.32	2	Steam-water mixture
260	1.8	6	Superheated steam
300	2	6	Superheated steam
320	2	6	Superheated steam

After hydrothermal treatment the furnace was allowed to cool down with the quartz tube inside. The quartz tube was then cut from the top using a diamond cutter and the crystallized water was taken out from the tube suspended in water. The aqueous suspension of the crystallized powder was ultrasonicated for 10 minutes and used for characterization. The different characterization techniques used are discussed later in this chapter

A schematic of the experimental set up is shown in fig 2.1.3. Two different cylindrical muffle furnace was used – one kanthal wire wound furnace while the other had silicon carbide heating elements. A PID controller was used for the temperature control of the furnace. Two thermocouples were used, one to indicate the temperature of the sample and the other to control the furnace temperature. The first thermocouple was placed next to the quartz tube and connected to a digital panel meter. The other thermocouple was placed adjacent to the furnace muffle to give a quick response for

better control. A difference of 20°C existed between the two locations, which was taken into account. The variation of the set point was only $\pm 1^{\circ}\text{C}$ when the silicon

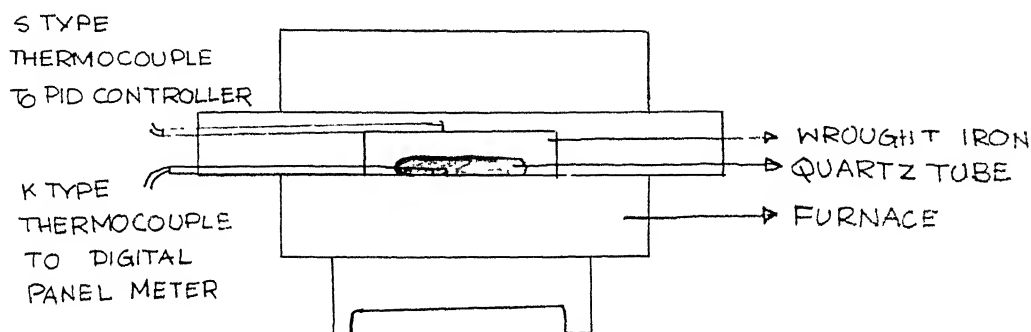


Figure 2.1.3. Schematic diagram of the furnace setup

carbide furnace was used and $\pm 0.5^{\circ}\text{C}$ when the kanthal wire wound furnace was used. The wrought iron tube was used for two purposes. First, the temperature homogeneity inside the wrought iron tube helped to maintain a single temperature around the quartz tube and secondly, it also saved the furnace muffle from any damage in the case of bursting of the quartz tube most probably due to the presence of any scratches etc which is known to decrease the strength of the tube drastically. Other possibilities include fatigue in the glass tube due to continuous heating at high temperature.

2.1.4. CALCULATIONS OF THE AMOUNT OF WATER REQUIRED TO GENERATE THE DESIRED PRESSURES

To start with the maximum pressure a quartz tube of definite diameter can withstand was calculated using the hoop stress. Hoop stress is defined as the

circumferential stress in a cylinder subjected to internal or external pressure and is given by

$$\sigma_n = pr/t$$

Where σ_n is the hoop stress, p is the pressure on the cylinder, r is the internal radius and t is the thickness of the cylinder. When subjected to internal pressure the hoop stress is tensile

The tensile strength of the quartz is ~50 MPa. Assuming a factor of safety 4 the maximum stress that can be generated without breaking the quartz tube is 12.5 MPa. The different quartz tubes available and the maximum calculated pressure that they can withstand are tabulated in table 2.1.3.

Table 2.1.3. Workable pressure for the tubes with different diameter and thickness

Internal diameter (mm)	Thickness (mm)	Maximum pressure (MPa)	Volume per unit length (ml/cm)
7	0.5	1.78	0.385
7	1.0	3.57	0.385
10	1.0	2.5	0.785
14	2.0	3.57	1.539
18	1.0	1.4	2.545
18	1.5	2.08	2.545
20	2.0	2.5	3.141

The smaller diameter tubes can withstand higher pressure but require larger length. The length of the tube should not exceed 15cm, the length of the hot zones of the furnaces. Taking all these factors into consideration the 18mm id, 1.5mm thickness quartz tube was chosen for hydrothermal crystallization.

Pressure inside the quartz tube was built up the autogenous steam pressure. As the maximum workable pressure is known suitable temperature, specific volume combination was find out by trial and error using steam tables and a steam table software. A typical calculation is described below. The pressure to be used is fixed to be ~2 MPa. An 18/21 mm quartz tube of 10 cm length was used for hydrothermal crystallization. So the available volume is 25.45 cc. The properties of superheated steam at 2 MPa are tabulated in table 2.1.3. The amount of water added to the dried

Table 2.1.3. Properties of superheated steam

Pressure = 2 MPa

Saturation temperature = 212.4°C

Temperature (°C)	Specific volume (cc/gm)	Mass of 25.45ml (gms)
220	102.2	0.249
230	105.4	0.241
240	108.5	0.235
250	111.5	0.228
260	114.4	0.222
270	117.3	0.217
280	120.0	0.212
290	122.8	0.207
300	125.5	0.203
310	128.2	0.199
320	130.8	0.195
330	133.4	0.191
340	136.6	0.187

gel should be sufficient to form at least a thick paste. Around 0.3 – 0.4 gms of powder is required to characterize a sample by SEM, particle size analysis, x-ray diffraction etc. About 0.2 cc of water is required to form a thick paste for 0.4 gms of powder. Assuming density of water to be 1gm/cc this amount of water is equivalent to 0.2 gms water. If this amount of water occupies a volume of 25.45cc the specific volume comes out to be 127.25cc/gm. The temperature of hydrothermal crystallization was decided to be 320°C. Using the steam table software the exact pressure for steam at 320°C and specific volume 127.25cc/gm was calculated to be 2.0532 MPa. On successive use the length of the tube decreases. Accordingly the amount of water required, powder to be added was recalculated to maintain the temperature, pressure values constant.

2.2 POWDER CHARACTERIZATION

The dried amorphous powder was characterized by Scanning electron microscope (SEM), BET surface area analyzer and x-ray diffractograms^{1.5m} (XRD), Thermogravimetric analysis (TGA) and Fourier transform infrared spectroscopy (FTIR). Precipitate dried without any washing was also prepared and characterized by XRD and Electron probe microanalysis (EPMA). Zirconia powders doped with 2, 5, 8, 10 mole percent gadolinia were prepared and hydrothermally crystallized at 270° C, ~1.80 MPa pressure for six hours. The powder was characterized by x-ray diffraction.

ZrO₂–10 mole% Gd₂O₃ was chosen for further investigation. The different conditions under which hydrothermal crystallization was done to study the different aspects of hydrothermal crystallization is tabulated in table 2.2.1 together with the

techniques used for characterization. The different instruments used for characterization are tabulated in table 2.2.2.

Table 2.2.1. Hydrothermal crystallization under different conditions

Conditions	Sample	Characterization	Aim
Hydrothermal crystallization at different temp. pressure for 6 hrs 200°C/~1.0 MPa 220° C/~1.6 MPa 260° C/~1.8 Mpa 300° C/~2.0 Mpa 320° C/~2.0 Mpa	HX 200 HX 220 HX 260 HX 300 HX 320	XRD, PSD	To find the lowest temperature, pressure of hydrothermal crystallization and their effect on particle size, crystallite size etc.
Hydrothermal crystallization at different pressures at 220° C for 6 hrs ~ 2.1 MPa ~ 1.56 MPa ~ 1.2 MPa	HP MP LP	XRD, SEM	To find the effect of pressure on hydrothermal crystallization
Hydrothermal crystallization of the amorphous powder with ultrasonication of the powder before hydrothermal treatment		XRD, PSD	To find if ultrasonication has any effect on the particle size of the crystallized product
Hydrothermal crystallization for different durations at 320° C and ~2.0 Mpa pressure PH=3 5 9 11	pH3 pH5 pH9 pH11	XRD PSD	To find how the particle size/ crystallite size changes with pH during hydrothermal crystallization

Hydrothermal crystallization at different steam/water ratio (done at high temperature saturated steam/water mixture instead of superheated steam) at 220° C/2.32 MPa /2 hours Steam : Water -----3:1 1:1 1:3		XRD	To find if at all presence of water at high temperatures leads to a different hydrothermal mechanism and its effect on the crystallite size
	HX/SW31		
	HX/SW11		
	HX/SW13		
Hydrothermal crystallization of amorphous powder with different particle sizes at 320° C/~2 MPa for 6 hours		XRD, PSD, SEM, TEM	To confirm the mechanism of hydrothermal crystallization

Amorphous powder was seeded with different amount of previously hydrothermally crystallized powders and hydrothermally crystallized at 320° C, ~2MPa for six hours. Seeds were also crystallized under similar conditions. The different hydrothermal seeding experiments done are tabulated below

Conditions	Sample	Characterization	Aim
0.5 % seeded 5.0 % seeded 50 % seeded	HX 320/5S HX 320/50S HX 320/500S	XRD, PSD, SEM	To study the mechanism of hydrothermal crystallization

Table 2.2.2. Different instruments used for characterization

Characterization technique	Model	Company
Scanning electron microscope	JSM – 840A	JEOL
X-ray diffraction	ISO DEBYEFLEX 2002	RICH. SEIFERT & CO.
BET surface area	SA3100	COULTER CORPORATION
Particle size analysis	ANALYSETTE 22	FRITSCH GmbH
Fourier transform infrared spectroscopy	VECTOR22	BRUKER

2.2.1. X-RAY DIFFRACTION

The phases present and the crystallite size were determined by the x-ray diffraction technique. X-ray diffraction pattern of the powder sample was taken with a RICH. SEIFERT ISO-DEBYEFLEX2002 diffractometer using CuK_α ($\lambda=1.54184 \text{ \AA}$) radiation with a monochromator. Specimens were made by packing the powder on a glass slide and the surface was smoothened by passing a glass slide back and forth. The powder was soaked with a few drops of methanol to stick it to the glass slide. For the x-ray diffraction of the particles in suspension specimens were prepared by putting a few drops of the suspension on a clean glass slide followed by drying in a microwave oven for 3 minutes.

The x-ray diffraction plots of the samples were taken between $2\theta=20^\circ$ and $2\theta=80^\circ$. The conditions of the diffraction are as follows.

Current, voltage	20mA, 30KV
Time constant	10 seconds
Beam slit width	2mm
Detector slit width	0.3 mm
Scanning speed	$3^\circ/\text{min}$ in 2θ
Full scale intensity	5,000 or 10,000 cpm

The intensity-angle data were recorded in a computer via an interface and latter plotted using a software. The peak position, corresponding relative intensities and the interplanar spacing (d) were obtained from the computer. The d values were calculated using the Bragg's formula

$$n\lambda = 2d \sin\theta$$

where n =order of reflection=1

λ =wavelength of reflection = 1.54184 \AA

d = interplanar spacing

θ =diffraction angle

The phase analysis and indexing of the peaks were done by matching the peak positions and the relative intensities with standard data (JCPDS files).

2.2.1.1 CRYSTALLITE SIZE ANALYSIS

The average crystallite size analysis of powder was carried out using the Scherrer formula:

$$t = \frac{0.9\lambda}{\beta \cos \theta}$$

where t = crystallite size

λ =wavelength of the radiation

β =corrected full width at half maximum (FWHM)

θ =diffraction angle

The intensity-angle data for each plot was retrieved from the computer, replotted and analyzed using a graphical software called ORIGIN5. Only cubic zirconia was obtained for the ZrO_2 -10mole% Gd_2O_3 composition and the crystallite size of this phase was calculated. The (111) peak of the cubic phase was used for the crystallite size analysis.

The uncorrected FWHM (B_o) measured from the plots has several components other the broadening due to crystallite size. They are

1. Instrumental broadening
2. Broadening due to spectral width i.e. the x-ray itself consists of two components having slightly different wavelengths
3. Broadening due to stress in the crystal

The instrumental broadening has also several components like broadening due to surface roughness of the sample, transparency of the sample, misalignment in the diffractometer etc.

As the powder was made from solution the crystallites are assumed to form without any constraints and therefore there is negligible strain in the crystals. So no correction was required for the broadening due to the strain in the crystal. For the correction of the broadening due to the spectral width the following procedure was followed. Figure 2.2.1³² was used to find the $K\alpha$ doublet separation, d at the 2θ value of interest. Knowing d and B_0 , the uncorrected FWHM for the sample, the value of B , the half width corrected for $K\alpha_1$ - α_2 broadening was determined from figure 2.2.2.³² To correct for the instrumental broadening the x-ray diffractogram of strain free, coarse silicon powder was obtained under similar conditions. The half widths of the peaks for (111), (220), and (311) corrected for spectral width was obtained as for the sample. This is called 'b'. It is plotted against 2θ (figure 2.2.3) and the value of b at 2θ corresponding to the sample peak is read from the plot. Now we have B and b , the corrected widths of the sample and the silicon respectively. Then figure 2.2.4³² is used the values of β/B corresponding to the value of b/B obtained as above. β is the desired half width after correction for structural width and instrumental broadening. This β is used in the Scherrer's formula to determine the crystallite size.

2.2.2. SCANNING ELECTRON MICROSCOPY (SEM)

Samples for the SEM characterization was prepared by depositing the powder particles on brass stubs. The stubs were polished to $0.05\mu\text{m}$ finish using alumina powder. They were thoroughly cleaned with water followed by acetone to remove any

foreign particles. A thin film of a cationic surfactant, Percoal 728, was formed on the polished surface of the stubs by dipping it in a solution of the surfactant for 1 minute. The stubs were taken out slowly and then shaken a few times to remove any extra solution. Then they were covered with a petridish with enough space so that the film remains untouched and dried at room temperature. After drying a drop of the suspension of the powder to be studied was put on the stub by means of a micropipette and allowed to dry under a lamp. After that a gold coating was formed over it by sputtering for 20 minutes in a coating unit (International Scientific Instruments PS2 Coating unit). A vacuum better than 10^{-1} mbar was maintained during sputtering. Gold coating makes the surface conducting ensuring a conduction path for the incident electrons. The particle size and morphology were viewed through a JEOL JSM840A scanning electron microscope. All the sample micrographs were taken in secondary mode.

The cationic surfactant was prepared as follows. 0.005 grams of the polymer was dissolved in 50ml (0.1 % solution) of water by stirring it for 5 hours. The solution was very viscous after the polymer has dissolved in it. As the polymer has a shelf life of few days after dissolution it was prepared every time when SEM was done.

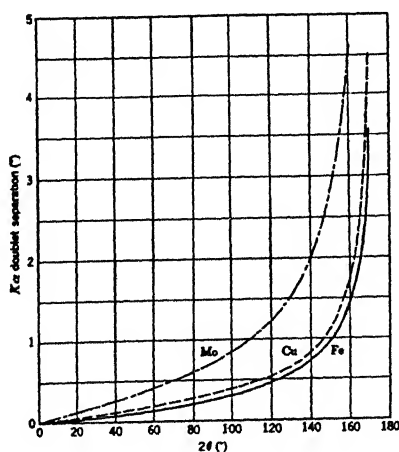


Figure 2.2.1. Angular separation of the $K\alpha$ doublet as function of $2\theta^{32}$

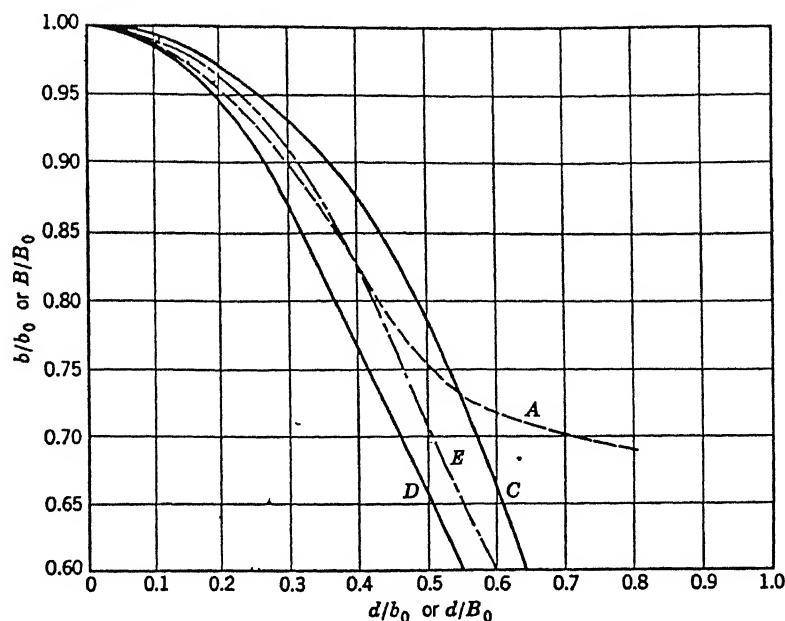


Figure 2.2.2. Curves for correcting line breadths for the $K\alpha$ doublet broadening

A \rightarrow Jones correction curves, C & D \rightarrow for Gaussian & Cauchy type distribution

E \rightarrow for profiles intermediate between Cauchy and Gaussian type profiles³²

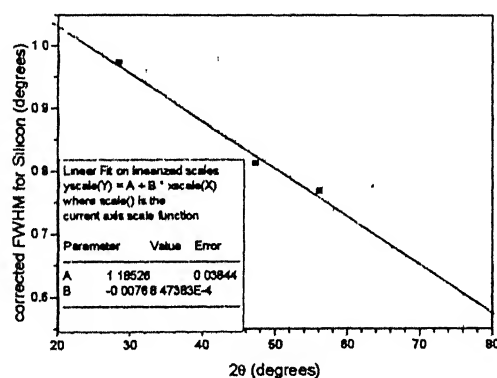


Figure 2.2. 3. Corrected full width at half maximum for silicon as a function of diffraction angle³²

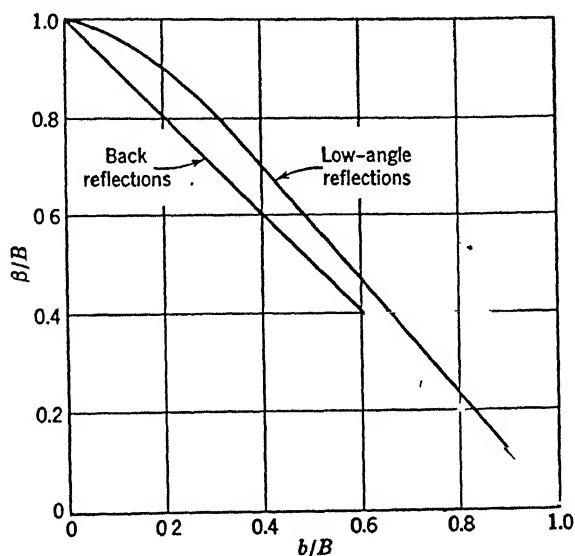


Figure 2.2.4. Curves for correcting x-ray diffractometer line breadths for instrumental broadening under conditions of high resolution³²

2.2.3. BET SURFACE AREA MEASUREMENT

The surface area was measured using a COULTER SA3100 instrument. The adsorbent gas used was dry nitrogen and carrier gas was helium. A weighted amount of the sample was first degassed at 120°C for 30 minutes and then weighed again to determine the losses. The tube containing the sample was then evacuated and maintained at liquid nitrogen temperature by putting it in a flask filled with liquid nitrogen. Dry nitrogen gas was allowed into the tube and the adsorption isotherm was observed. Then the liquid nitrogen flask was removed. The sample tube came to the

room temperature and the desorption isotherm was observed. The surface area was then calculated from the adsorption and the desorption isotherm using BET equation.

2.2.4 PARTICLE SIZE ANALYSIS

A particle size analyzer Analysette 22 of FRITSCH GmbH was used to measure the particle size distribution. All the powders used for particle size analysis were suspended in water and ultrasonicated for 10 minutes before particle size analysis. The suspension was poured in a distilled water filled vessel under constant stirring and ultrasonication until its concentration is ~10 % as shown by the computer interfaced with the instrument. Then the suspension was pumped through a cylindrical chamber fitted with lenses. A helium-neon laser beam was allowed to pass through the chamber. The laser beam was diffracted by the particles in the suspension. The diffraction pattern is recorded in a computer interfaced with the analyzer and the particle size is determined from it by some complex mathematical calculations.

3 Results and Discussions

3.1 OPTIMISATION OF UREA HYDROLYSIS PROCESS

Hydrolysis of Zr and Gd salts in aqueous solutions was carried out using urea. The conditions of hydrolysis such as “with” or “without refluxing”, specific molar ratio of urea to salts, pH, temperature, nature of salts was varied. The results are described and discussed in this section.

In the first set experiments, the hydrolysis experiments were carried out by heating the aqueous solution either in a covered beaker without refluxing or with refluxing in round bottom flask fitted with reflux condenser. In each case 14.5 gms of $\text{ZrOCl}_2 \cdot 8\text{H}_2\text{O}$ and 1.8 gms Gd_2O_3 was stirred with enough water to make 100ml solution. This corresponds to 10 mole percent gadolinia in zirconia. Different amounts of urea were added. On heating, a white precipitate appeared after sometime. This time was noted. The heating process was continued for six hours. The heating was carried out at the boiling temperatures of the solutions in all cases except in one case

when the temperature was kept below 100°C . The results are given in table 3.1. The time for the precipitate to appear is plotted against urea/salt ratio in fig 3.1.1.

Table 3.1.1. Time for precipitation in urea hydrolysis of 0.5m/l ZrO_2 -10 mole % gadolinia containing different amounts of urea

Urea content (gms)		Refluxing?	Temperature ($^{\circ}\text{C}$)	Time for precipitation (mins)
(Gms)	SMR			
27	~9	No	~105	50
21.6	~7.2	No	~105	65
16.2	~5.4	No	~105	55
10.8	~3.6	No	~105	72
5.4	~1.8	No	~105	115
	0.5	Yes	~105	600
	1	Yes	~105	190
	1	Yes	<100 $^{\circ}\text{C}$	Precipitate didn't appear even after 12 hours of heating
	2	Yes	~105	~180

Theoretically the amount of urea required to hydrolyse one mole of salt is 0.5 moles i.e. $\text{SMR} = 0.5$. With this amount of urea, the precipitate was obtained only after 10 hours of heating. The time decreased rapidly on increasing the urea content to ~1 hour at $\text{SMR} = 3.6$. It didn't change further with additional increase in SMR (fig. 3.1.1). When hydrolysis experiment was carried out at $<100^{\circ}\text{C}$, much longer time was required for the precipitation (table 3.1.1). A thick gelatinous precipitate was obtained when urea hydrolysis was done with urea content corresponding to 1 at the boiling temperature of the solution. The final pH was ~4 after 6 hours of heating. When urea hydrolysis was done under refluxing with higher urea content ($\text{SMR}=2$), a thick precipitate with a clear supernatant liquid was obtained on cooling from its boiling

temperature. In addition, the final pH was somewhat higher (~5). This made the separation of the precipitate and further processing easier. So further urea hydrolysis were all done with $SMR = 2$.

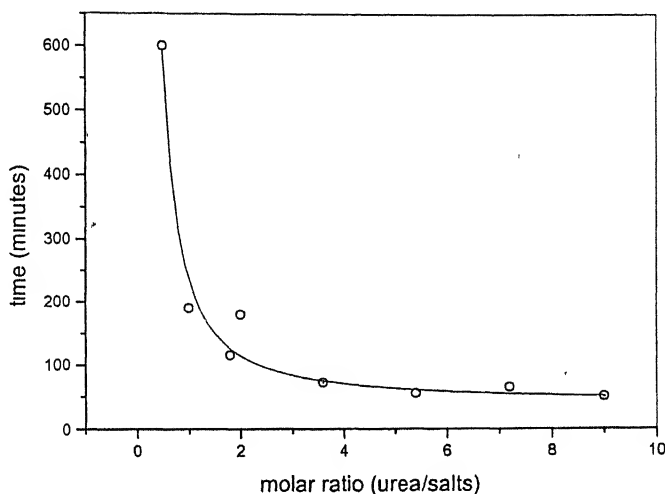


Figure 3.1.1 Time for precipitation in urea hydrolysis of 0.5m/l ZrO_2 -10 mole % gadolinia containing different amounts of urea

The time required for precipitation was same whether the addition of urea as powder or as solution to the salt solution. Hydrolysis was most effective when urea was added to the salt solution that had been already boiling for 1 hour. Earlier addition of urea resulted in the formation of urea hydrochloride salt, leaving reduced amount of urea available for hydrolysis. The boiling of urea solution before addition of salts led to the partial decomposition of urea.

In the above experiments, gadolinium was added as Gd_2O_3 powder. It was expected that the strong acidic conditions provided by $ZrOCl_2 \cdot 8H_2O$ solution would be sufficient to dissolve Gd_2O_3 . However, the x-ray diffractograms of the hydrolysis product revealed the material to consist of an amorphous phase together with

crystalline zirconia. Thus, gadolinia is not going into solution in the above experiments.

Similar experiments were performed by using nitrate and chloride as source of gadolinium. Nitrate and chloride of gadolinium was prepared by dissolving Gd_2O_3 in 1.1 nitric acid and hydrochloric acid respectively. After the hydrolysis, the supernatant mother liquor and the wash effluent were dried. The solid residue was heated at $900^{\circ}C$ for two hours and x-ray diffractograms was taken to determine the phases. The results are tabulated in table 3.1.2.

The results clearly show that gadolinium when added as nitrate forms solid solution with zirconia most effectively. Hence, in all further experiments gadolinium nitrate was used as the source of gadolinium.

Table 3.1.2. Effect of different gadolinia content on the urea hydrolysis

Gadolinium salt	$Gd(NO_3)_3$	Gd_2O_3	$GdCl_3$
<div>Urea</div> <div>————— molar ratio</div> <div>$(ZrO_2 + Gd_2O_3)$</div>	2	2	2
Gadolinia content	10	10	10
Residue	Very small amount of residue; residue is mostly gadolinium zirconium oxide	Large amount of residue; residue is cubic gadolinia	Large amount of residue; residue is cubic gadolinia

The variation of pH during urea hydrolysis (SMR =2) of zirconium oxychloride and gadolinium nitrate was also observed to elucidate the mechanism of urea hydrolysis. The results are shown in figure 3.1.2. Initially at the start of heating of the salt solution, the pH is 0.85. The pH decreases with time as the hydrolysis reaction proceeds. After 1 hour, as the urea solution is added the pH increases to 1.5 from 0.56. The pH decreases to its equilibrium value again with time. After about 90 minutes, the pH starts increases very slowly at a constant rate. It is only after about 230 minutes the pH increases very sharply indicating very fast decomposition of urea followed by decrease in rate and ultimately the pH reaches around five, which changes only slightly with time.

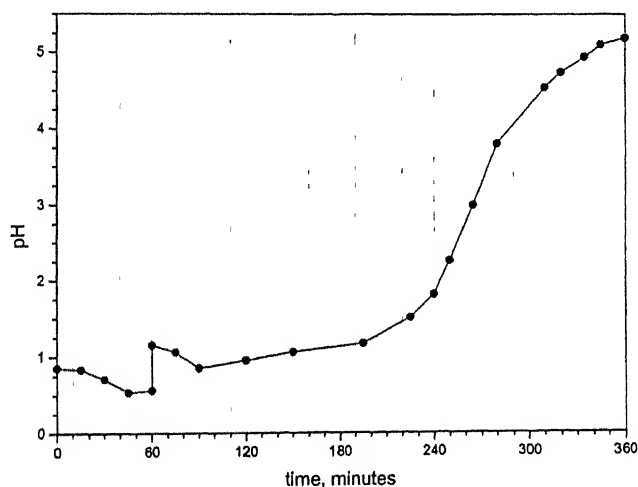


Figure 3.1.2. Variation of pH with time during urea hydrolysis

In the initial trials, the whole of the suspension (precipitate and the liquid) after urea hydrolysis was dried by keeping in an oven at 100°C for 8 hours. The x-ray diffractograms of this product is shown in figure 3.1.3a. The product was crystalline but couldn't be identified. If the product was dried for 24 hours at 150°C then it becomes amorphous (figure 3.1.3b). Similarly, if the precipitate was separated from

the suspension by centrifuging and then washed several times with deionised water and propanol followed by drying at 80°C for 8 hours, then also it was found to be amorphous (figure 3.1.3c) Based on this experiments it is suspected that the crystalline phase in the dried hydrolysis product is due to the presence of chlorine. Electron Probe Micro Analysis (EPMA) of this powder showed the presence of large amount of chlorine (figure 3 1.4).

In an attempt to see if the nature of the hydrolysis product changes with time for which the hydrolysis is carried out, the hydrolysis reaction was carried out for 70 hours. Figure 3.1.5 gives the x-ray diffractograms of the 100°C dried hydrolysis product (without washing). The same unknown crystalline phase was obtained and its nature doesn't change much with the hydrolysis time.

product (without washing). The same unknown crystalline phase was obtained and its nature doesn't change much with the hydrolysis time.

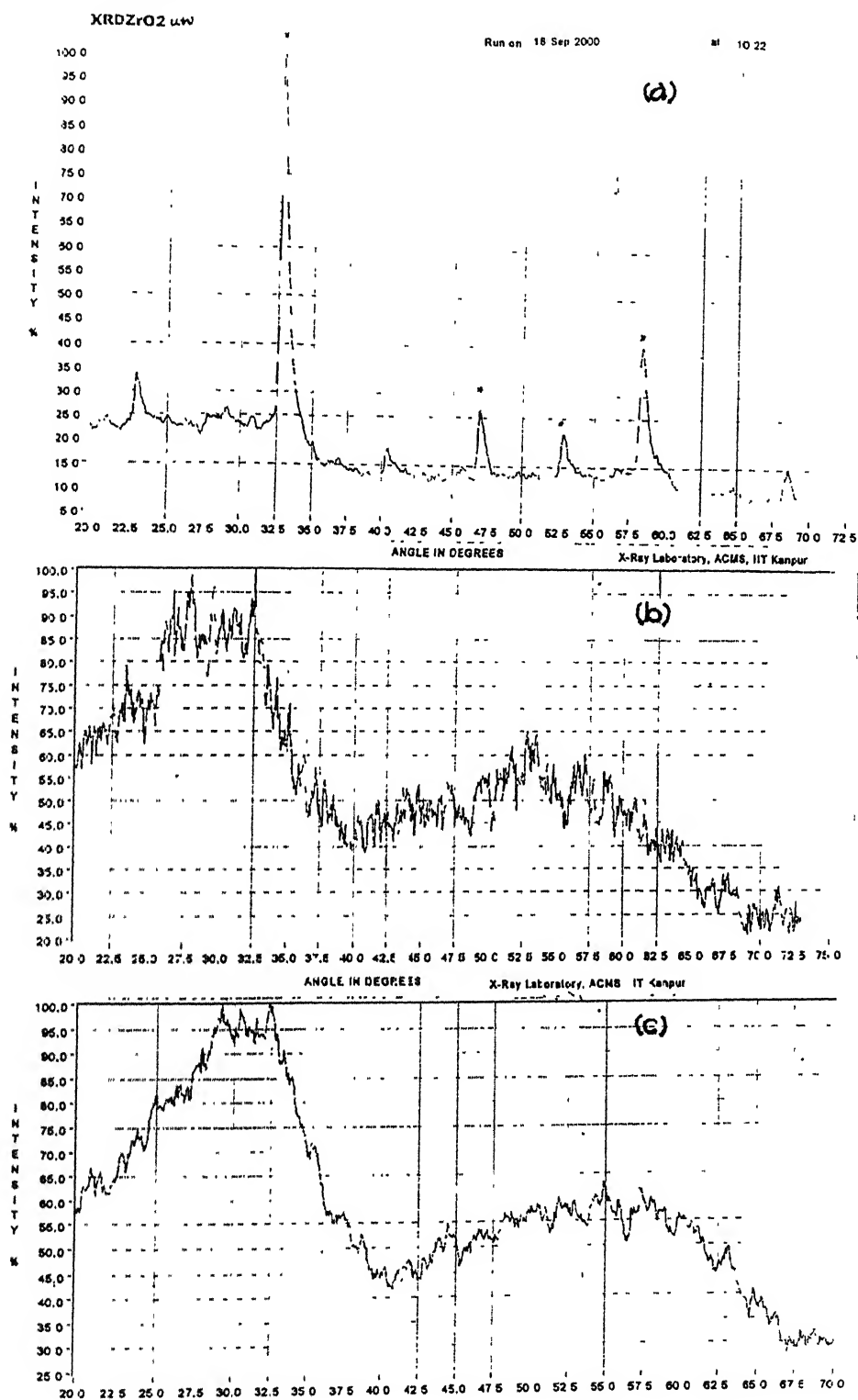


Figure 3.1.3. X-ray diffraction plots for the hydrolysis product under different conditions (a) hydrolysis product dried at 100°C for 8 hours, (b) same powder after drying at 150°C for 24 hours, (c) hydrolysis product after removal of chlorine

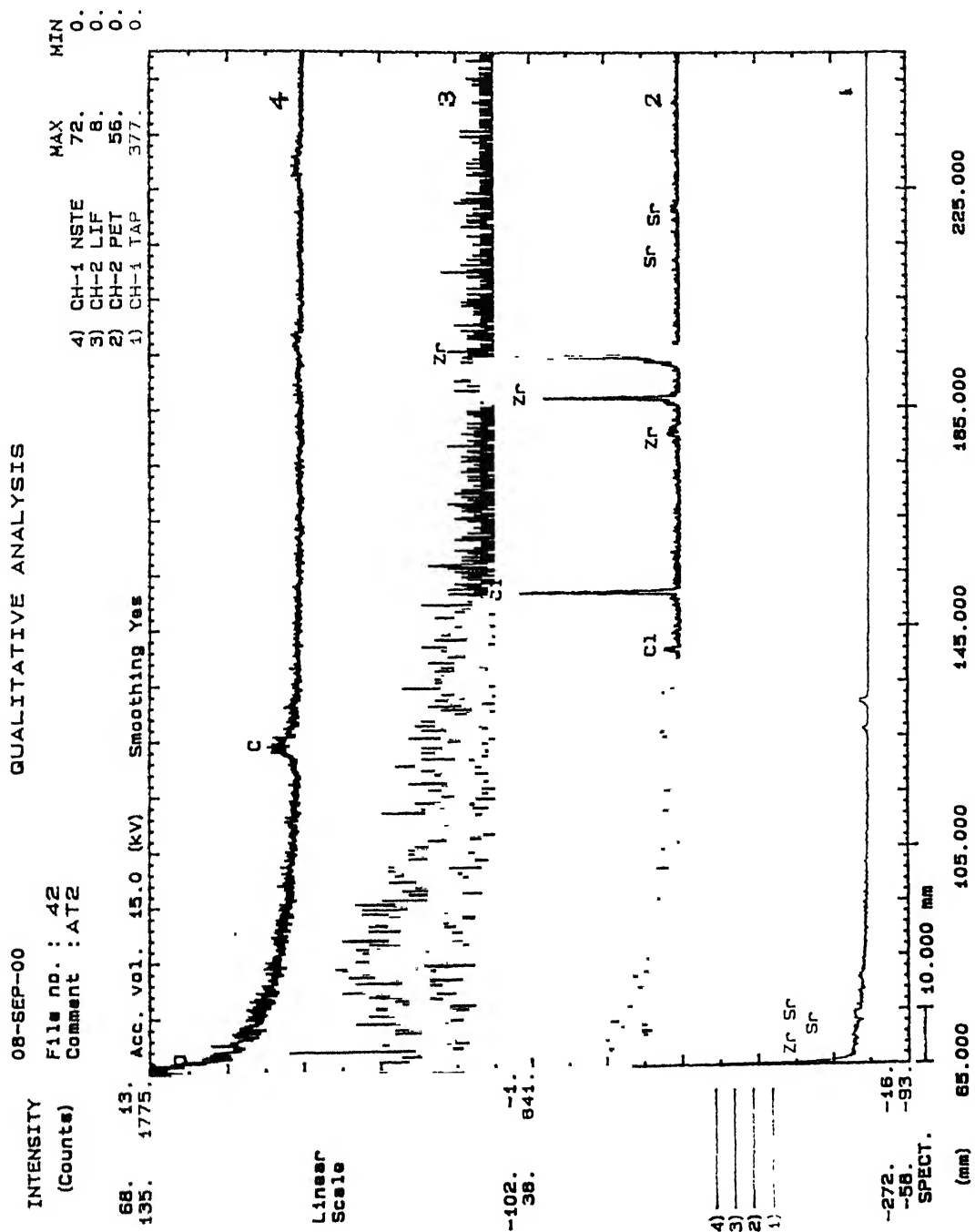


Figure 3.1.4. Electron probe microanalysis of the dried hydrolysis product obtained after urea hydrolysis

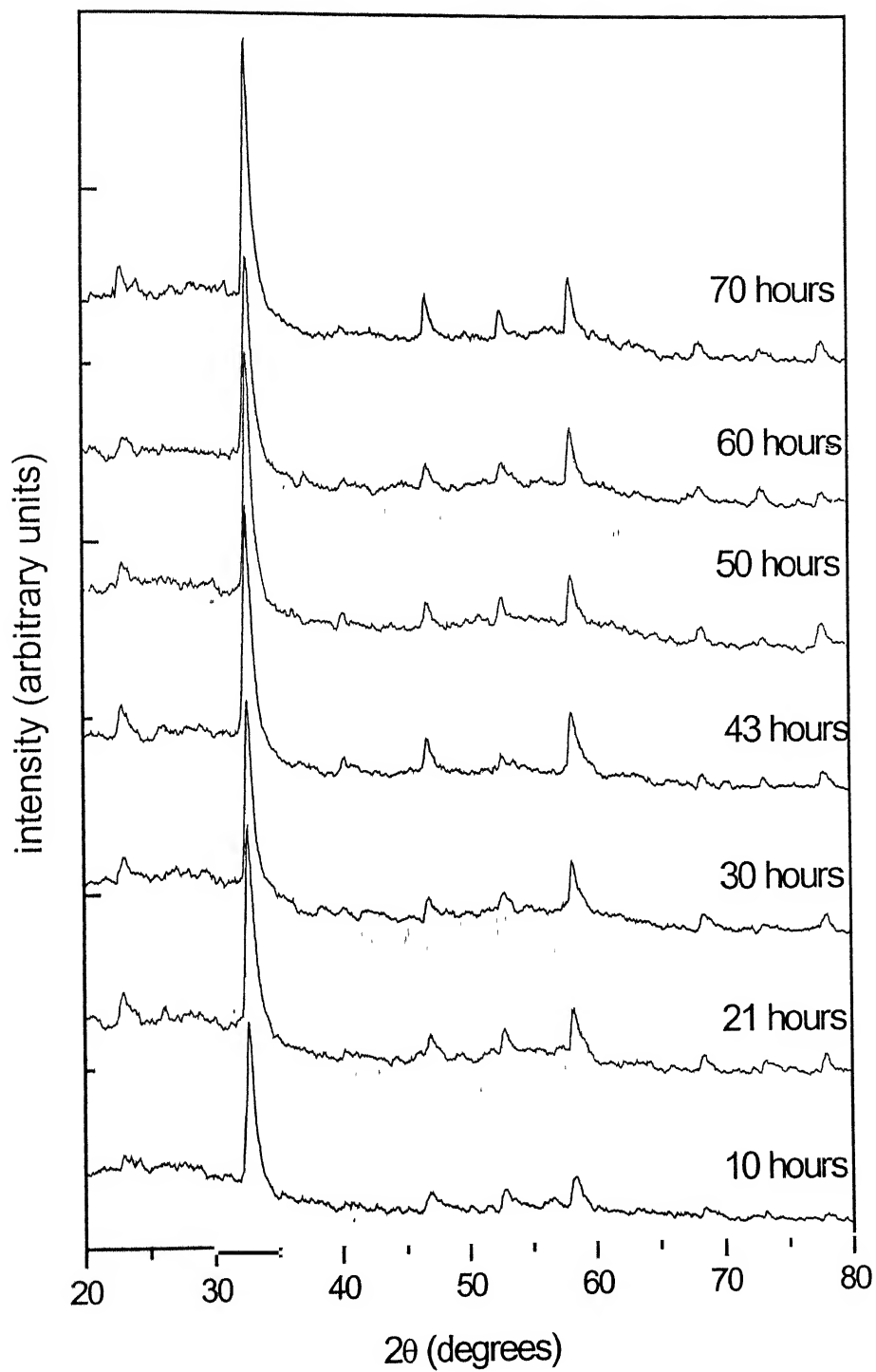


Fig 3.1.5. X-ray diffractograms of powders sampled out after different periods of urea hydrolysis as mentioned in the figure

3.1.1. PROPERTIES OF AMORPHOUS POWDER OBTAINED AFTER UREA HYDROLYSIS

As described in the later section detailed studies were done on the 10 mole percent gadolinia- zirconia composition. Hence, the results of the amorphous powder prepared by the urea hydrolysis of this composition are described here. Other compositions also had similar properties. The powders were washed and dried as discussed in chapter 2. Figure 3.1.6 (a) and (b) gives the examples of the limiting particle size distributions obtained in hydrolysis product. It is seen that the distribution is bimodal in which the relative heights of the two peaks vary substantially from run to run. The particle size ranges from 0.1 μm to as high as 35 μm with the two peaks occurring at about 1.3 μm and 13 μm .

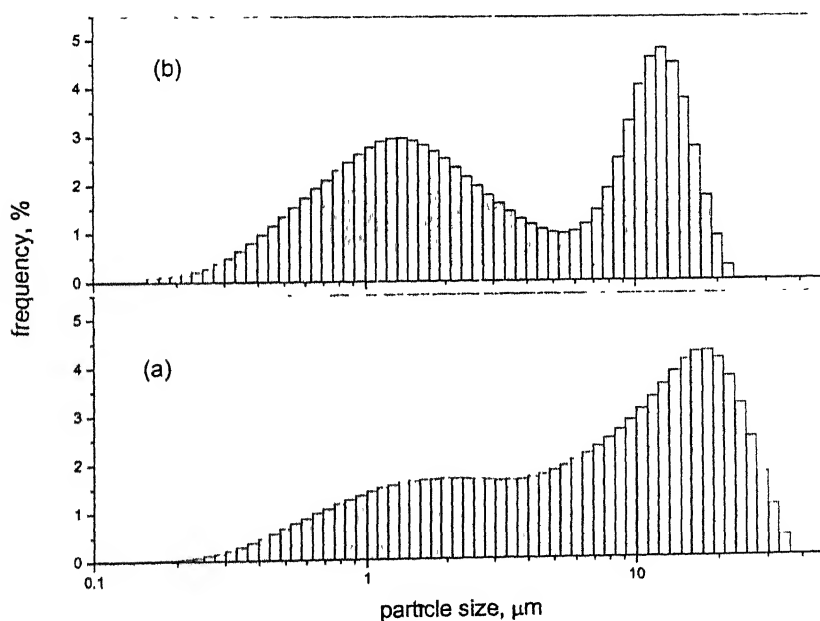


Figure 3.1.6. Limiting particle size distributions of the amorphous powders

The surface area of the powder is $\sim 245 \text{ m}^2/\text{gm}$. This corresponds to an elementary particle size of $\sim 2 \text{ nm}$ assuming a spherical shape. These results indicate

that the particles are highly agglomerated. Figure 3.1.7 represents the X-ray diffractogram of the amorphous powder. The X-ray diffraction pattern of the amorphous powder shows gross amorphous structure with two broad humps centred around $2\theta = 30^\circ$ and 54° degrees. Figure 3.1.8 shows the TGA of the amorphous powder. The FTIR spectrum of the amorphous powder is shown in figure 3.1.9. For comparison TGA and FTIR of a crystalline powder hydrothermally treated at 320°C , $\sim 2\text{Mpa}$ for six hours is also given along with that of amorphous powder in the figures.

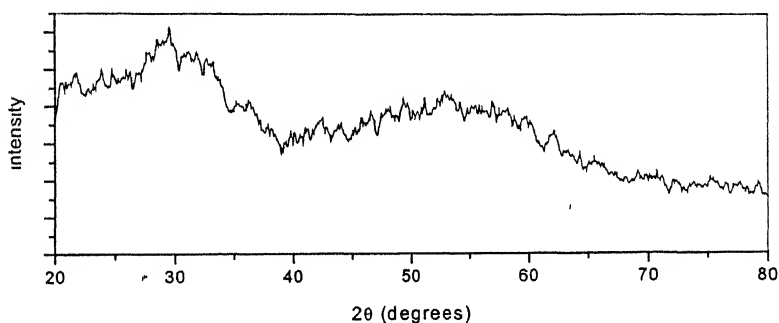


Figure 3.1.7. The x-ray diffractogram of the amorphous powder

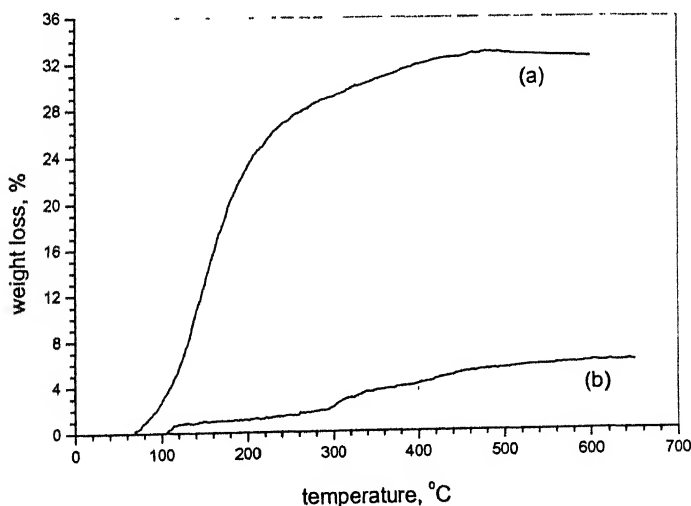
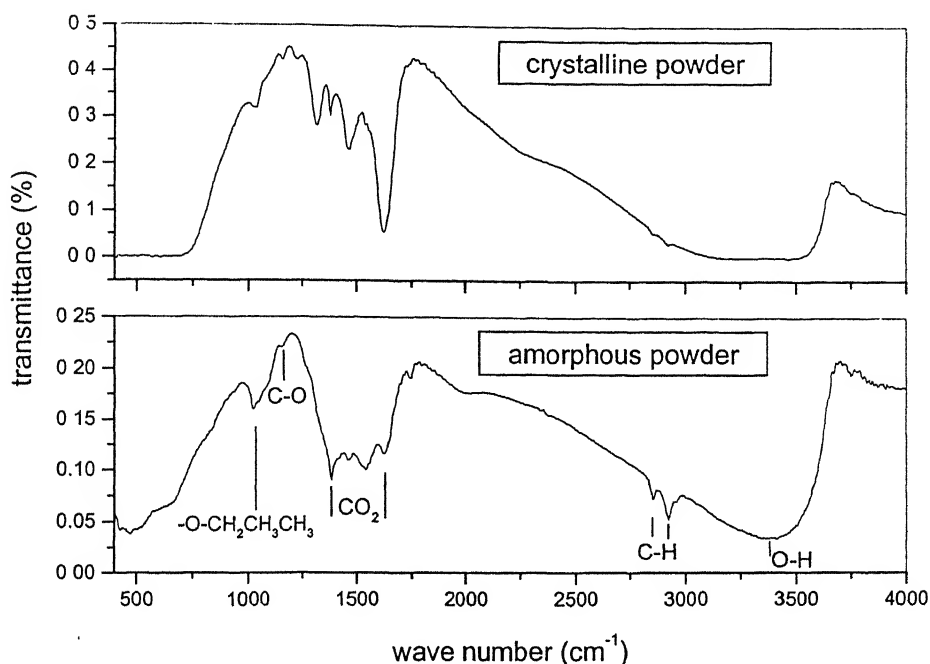


Figure 3.1.8. Thermo gravimetric analysis of (a) amorphous powder and (b) crystalline powder



**Figure 3.1.9 FTIR spectrum of the amorphous and crystalline powder
hydrothermally crystallized at 320°C, ~2 MPa for 6 hours**

The TGA plot of the amorphous powder follows a sigmoidal pattern with an initial incubation period up to ~70°C. There is a little loss (~4 %) up to 120°C showing that only a small amount of water and free alcohol are present in the powder. This is expected as the urea hydrolysed powder was dewatered with n-propanol before drying. After 120°C, the loss curve follows a relatively steep slope with a total loss of 33% by weight on heating up to 600° C. There is a loss of about 29% between 120°C and 400°C. This is most probably due to the removal of surface adsorbed propanol molecules. The fact that there is propanol associated with the powder is evident from the FTIR spectra as described below. After 400°C, there is almost no loss in weight up to 600°C. On the other hand, the crystalline powder has a total loss of only 6% when heated up to 650°C. There is only about 1% loss up to 120°C showing only a small

amount of free water present in the powder. The powder shows no loss in weight below 100°C. This is expected as the powder was dried at 100°C prior to the experiment. The little loss (2%) up to 300°C in the crystalline powder indicates that there is only a small amount chemically adsorbed alcohol in the powder. The FTIR results described below also supports this result. There is a sudden change in slope after 300°C showing a loss of about 4% between 300°C and 650°C. This might be due to the removal of chemically bonded water molecules that got attached to the powder during the hydrothermal treatment.

In the FTIR spectra, the extensive interaction of the powder with propanol is shown by bands at 1022 cm^{-1} due to C-O stretching from chemically adsorbed propanol. The bands around 1384 cm^{-1} and 1460 cm^{-1} are due to surface adsorbed carbonate groups. The bands at 1620 cm^{-1} and 3411 cm^{-1} are due to O-H bending and stretching vibrations respectively. The bands around 2923 cm^{-1} and 2853 cm^{-1} are due to C-H bond. The absence of bands around 1022 cm^{-1} and reduction of the 2923 cm^{-1} and 2853 cm^{-1} supports the removal of alcohol after the hydrothermal treatment. The increase in the intensity of 1620 cm^{-1} peak shows increased association of O-H bonds with the powder. This might be due to the presence of water in the sample due to improper drying or handling during pellet making or increased association of water during hydrothermal treatment. The appearance of peaks around 1034 cm^{-1} , 1159 cm^{-1} and 1231 cm^{-1} in the FTIR spectrum of the crystalline powder cannot be accounted for. They might be due to some association of gadolinium.

3.2 HYDROTHERMAL CRYSTALLIZATION

The product of urea hydrolysis was subjected to hydrothermal treatment. The conditions used for the preparation of the amorphous powder are given in table 3.2.1.

Table 3.2.1. Conditions of the preparation of amorphous powder used in hydrothermal crystallization

Starting materials	ZrOCl ₂ . 8H ₂ O, Gd ₂ O ₃ , Urea
Temperature	105°C
Time	6 hours
Separation of solid product	Centrifuging at 5000rpm for 30 minutes followed by decanting of the mother liquor from the precipitate
Washing	Repeated cycles of stirring with DI water followed by separation of the wash water by centrifuging until the powder was free of chlorine
Drying	At room temperature for some time followed by drying in oven for 8 hours at 80°C

Amorphous powder containing 10 mole % Gd₂O₃ was used in the initial experiments. Weighted amount of powder with calculated amount of water was sealed in a quartz tube, which was then kept at different temperatures for 6 hours. The steam pressure generated inside the tube under these conditions depends on the water content and the temperature of hydrothermal treatment. Figure 3.2.1 shows the x-ray diffractograms of the resulting powders. After the treatment at 200° C, two broad peaks are seen centered at about $2\theta = 30^\circ$ and $2\theta = 54^\circ$ (fig a) The treatments at higher temperatures produced well-developed peaks, which match with the cubic phase of the zirconia. Thus, the hydrothermal treatment is successful in synthesising Gd₂O₃ doped ZrO₂ powder, which, as discussed earlier, is difficult to synthesise by other methods. The peaks become sharper as the crystallization temperature is increased. The presence of

a higher background intensity in the diffractograms of the samples treated at lower temperatures indicates that some amorphous phase may be present at temperatures up to 300°C. At the highest temperature used i.e. 320°C the background intensity is lowest and peaks are sharpest. Correspondingly, the crystallite size as measured from the broadening of the (111) peak using Scherrer formula increases with the treatment temperature (Table 3.2.2).

Table 3.2.2 The Effect of the hydrothermal treatment condition on the crystallite size

Temperature (°C)/ Pressure (MPa)	Crystallite size (nm)
220/1.6	27
260/1.8	28
300/2	62
320/2	55

Fig 3.2.2 shows the particle size distributions of the amorphous gel powder and the powder crystallized under various conditions. The particle size distributions of the crystallized powders are very similar to those of the amorphous powder. The apparent difference in the particle size distribution of the sample treated at 260°C appears to be a sampling problem. This indicates that the particle size of the phase remains nearly unchanged upon crystallization. Fig 3.2.3 show the SEM photographs of the powder treated at 220°C/1.6 MPa for 6 hours. The larger particles are surprisingly compact.

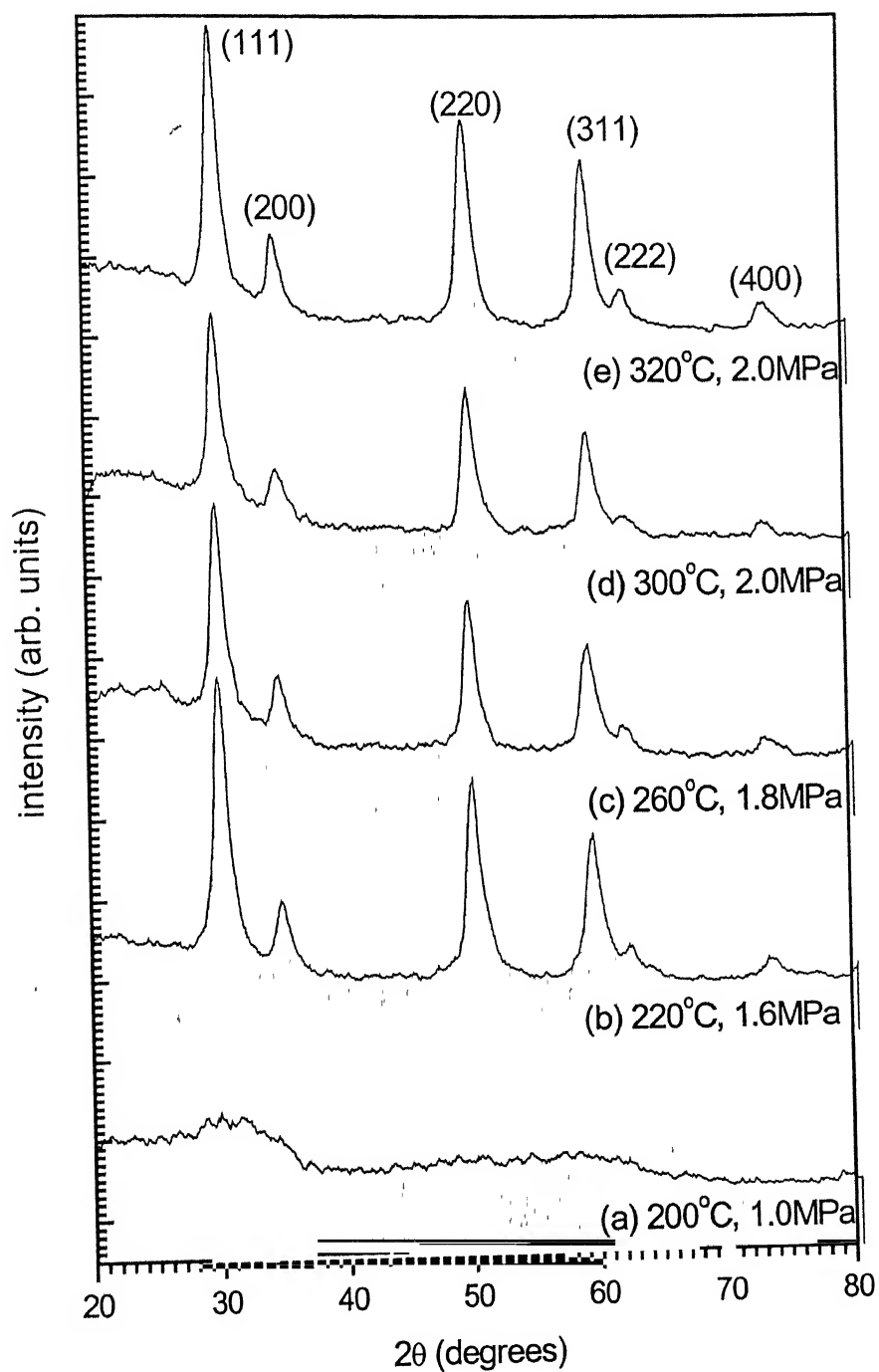


Figure 3.2.1 X-ray diffractograms from powders hydrothermally crystallized at different temperatures and pressures as mentioned in the figure

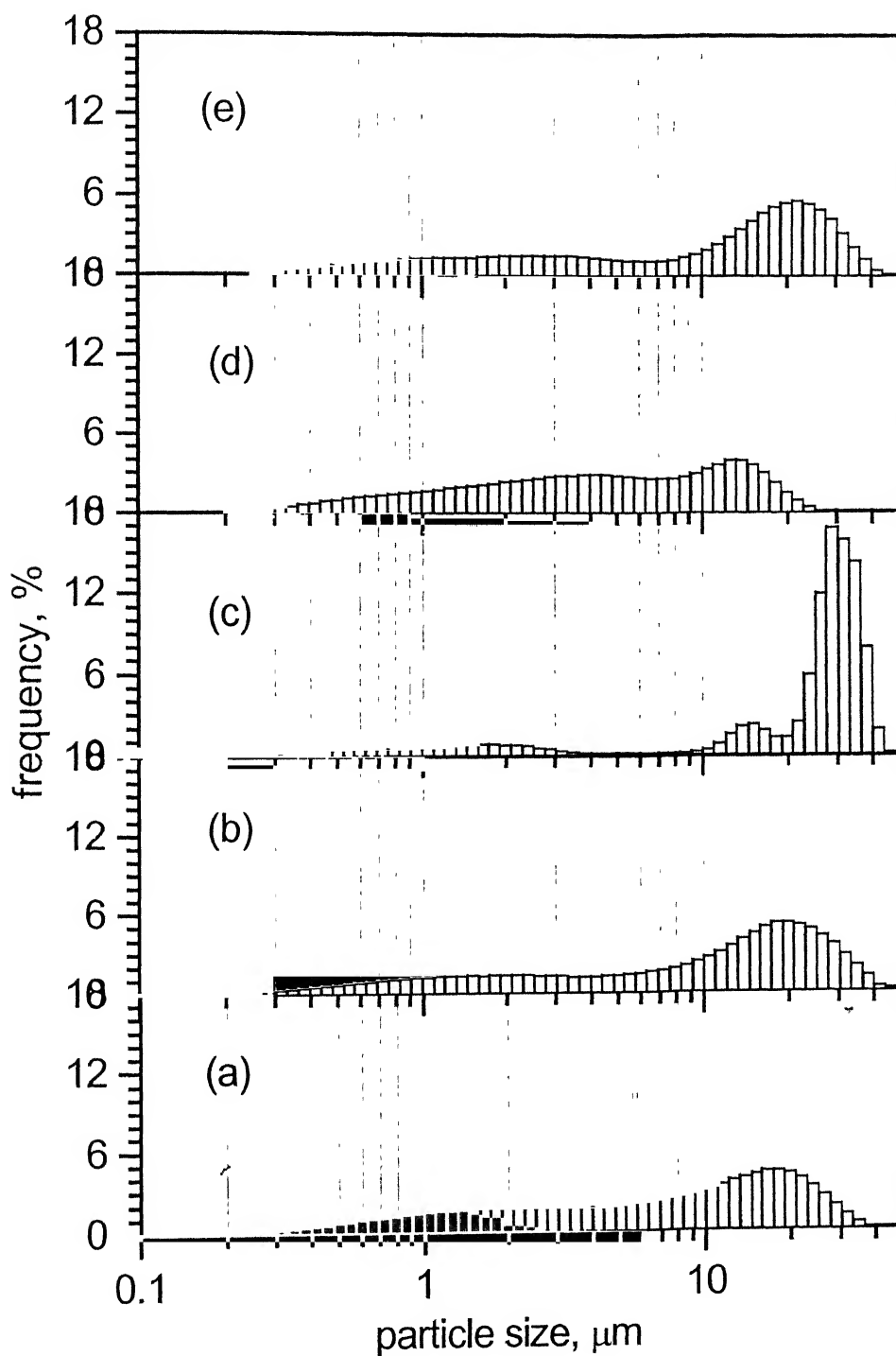


Figure 3.2.2 Particle size distribution of the (a) amorphous gel powder and the crystalline powders obtained from it by hydrothermal treatment at (b) 220°C, 1.6 MPa, (c) 260°C, 1.8 MPa, (d) 300°C, 2.0 MPa, and (e) 320°C, 2.0 MPa



Figure 3.2.3. SEM image of the powders hydrothermally crystallized at 220°C, 1.6

The above experiments were carried out using water without any mineralizer. It is known that the solubility of zirconia in water is a strong function of pH. It has been proposed that the difference in solubility lead to the change in mechanism. To investigate this aspect we carried out the crystallization treatment at pH 3, 5, 9 and 11 at 320° C for 6 hours. The pH below 7 was achieved by the addition of nitric acid and those above 7 by adding ammonium hydroxide. The resulting particle size distribution is shown in figure 3.2.4. When the pH is in the acidic range, the particle size decreases after hydrothermal treatment at 320°C, ~2MPa pressure for 6 hours.

As the pH increases, the particle size distribution becomes spread over a larger region. The crystallite size as determined from the x-ray diffraction patterns is 45nm, 30nm, 30nm, and 31nm for powders treated at pH 3, 5, 9, and 11 respectively. Though the particle size changes there is virtually no change in the crystallite size with pH. The agglomeration of the crystallites is more at higher pH. The reason for this is not fully understood.

3.2.1. EFFECT OF GADOLINIA CONTENT ON THE HYDROTHERMALLY CRYSTALLIZED PHASES

Powders containing 2%, and 5% Gd_2O_3 was also prepared by hydrothermal treatment at 270°C, 1.8 Mpa for 6 hours of the corresponding precursors. When the gadolinia content is 2% and 5% only monoclinic phase is found to crystallize on hydrothermal treatment; whereas only cubic phase is found to crystallize when 8% and 10% gadolinia is added with zirconia (figure 3.2.5). No tetragonal phase was detected in any of the compositions – the peaks (004) and (220) at $2\theta = 71.56$ and 73.53 was not observed. While the results are as expected for other compositions, for

5 mole % Gd_2O_3 composition the tetragonal phase is expected but instead only monoclinic phase was obtained.

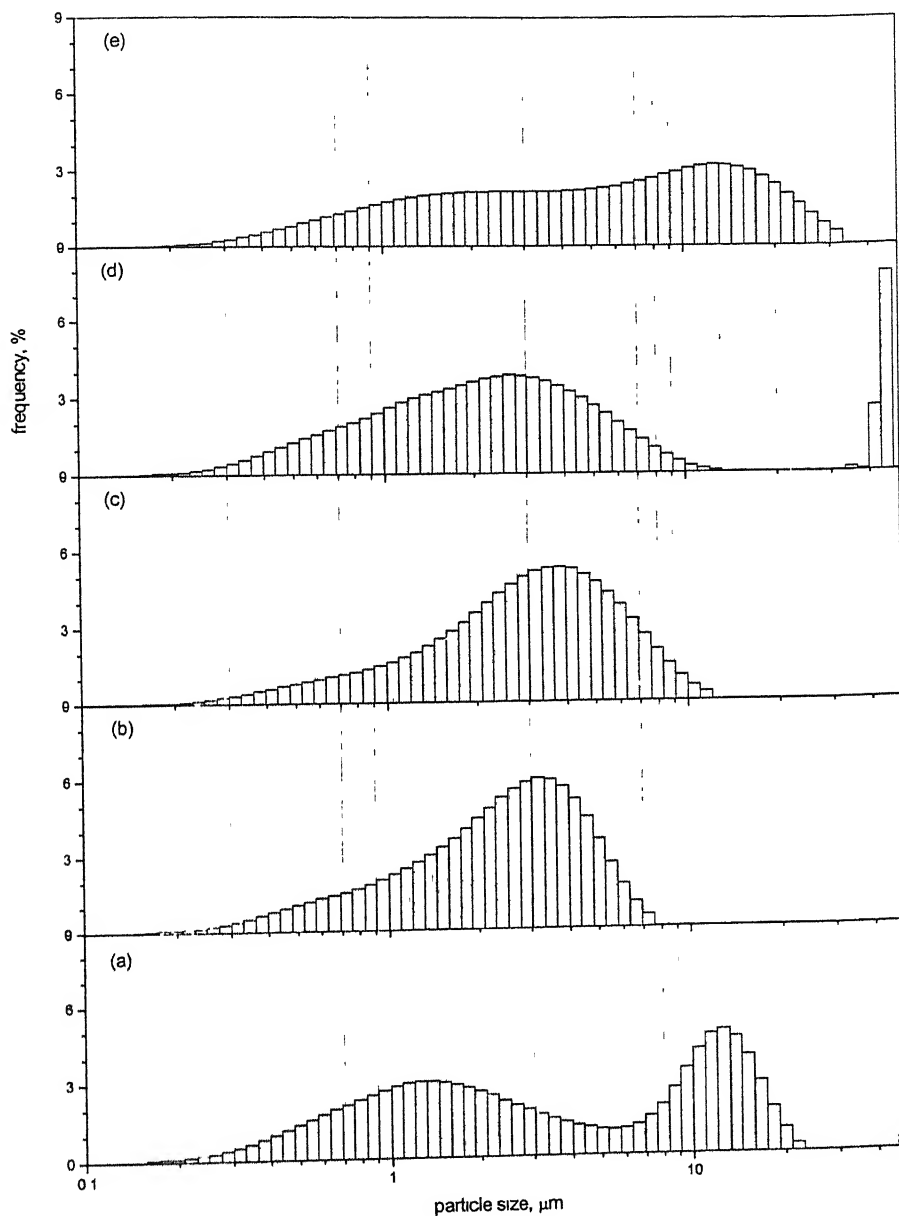


Figure 3.2.5. Particle size distribution of the (a) amorphous powder and the powders hydrothermally crystallized from it at 320°C, 2MPa for 6 hours at (b) pH 3, (c) pH 5, (d) pH 9, (e) pH 11.

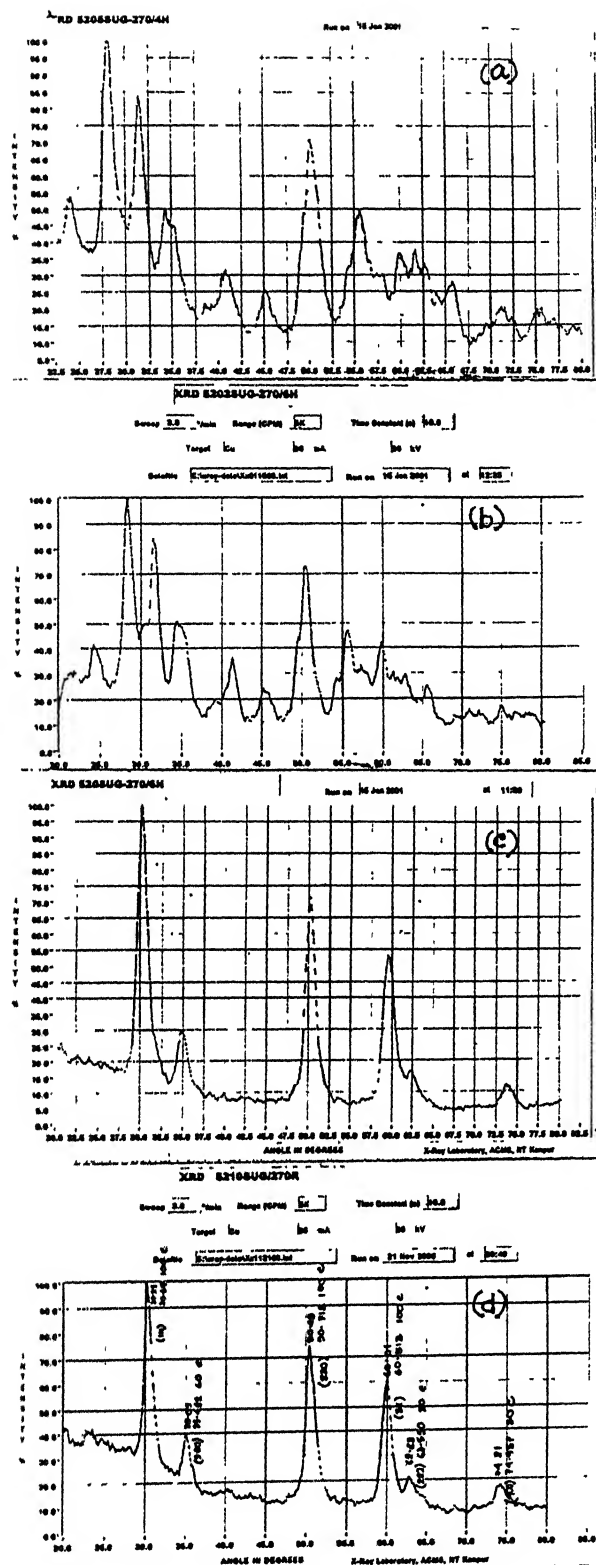


Figure 3.2.5. X-ray diffractograms of the zirconia powders after hydrothermal treatment at 270°C, ~1.8 MPa for 6 hours doped with different amounts of gadolinia; (a) 2 mole %, (b) 5 mole %, (c) 8 mole % and (d) 10 mole %

3.2.2 EFFECT OF HYDROTHERMAL TREATMENT PRESSURE

To determine the effect of pressure on the hydrothermal crystallization the amorphous gel powder was treated at 220°C for 6 hours at three different pressures - 1.3, 1.6, and 2.1 MPa. The corresponding X-ray diffractograms are shown in fig 3.2.6. There is a small but significant effect of pressure on the crystallization behaviour. The raised background level between $2\theta = 22^\circ$ to 37° indicates that some amorphous regions are still present in the powder treated at the lowest pressure. This feature is not present at the other two, higher pressures. The X-ray peaks also sharpen with increase in pressure. The crystallite sizes are 22, 27, 42 nm for 1.3, 1.6, 2.1 MPa pressure respectively.

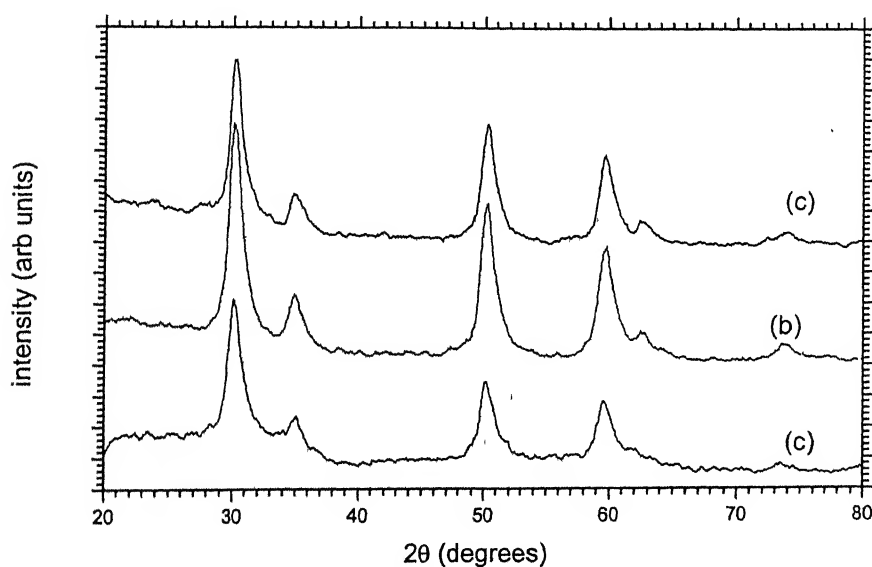


Fig 3.2.6. X-ray diffractograms from the powders hydrothermally crystallized at 220°C for 6 hours at pressures (a) 1.3 MPa, (b) 1.6 MPa, (c) 2.1 MPa

3.2.3 EFFECT OF HIGH TEMPERATURE STEAM-WATER MIXTURE ON THE HYDROTHERMAL CRYSTALLIZATION

In all the above experiments, the hydrothermal crystallization was done at superheated steam. The principal mechanism of hydrothermal crystallization seems to be topotactic nucleation and growth. To see if steam–water mixture at high temperature, pressure has any effect on the hydrothermal crystallization, experiments were performed at 220°C and 3.2 MPa pressure for 2 hours. The ratio of steam to water was varied. The x-ray diffractions patterns were shown in figure 3.2.7.

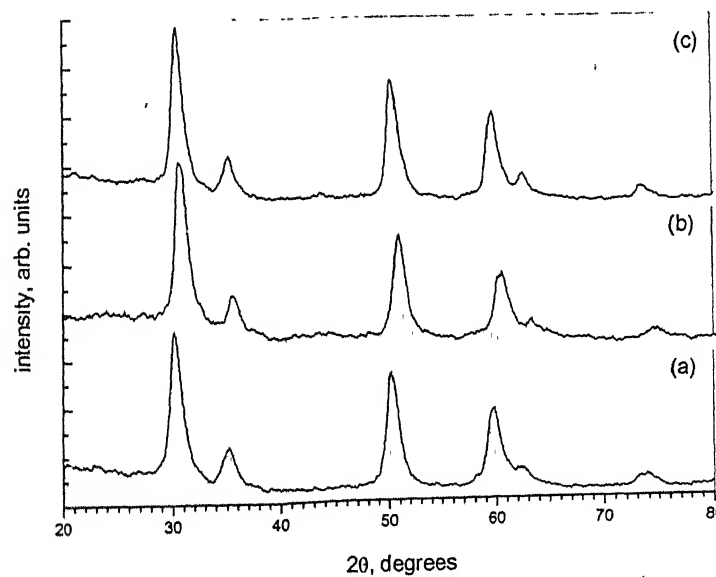


Figure 3.2.7. X-ray diffractograms of the powders after hydrothermal crystallization at a temperature of 220°C, 2 MPa pressure for 2 hours with steam to water ratio of (a) 3:1, (b) 1:1, (c) 1:3

The powder has crystallized within 2 hours of hydrothermal treatment into pure cubic phase. At the same temperature crystallization of the amorphous powder occurred in 6

hours when hydrothermal treatment was done under superheated steam pressure of 1.6 MPa. It clearly indicates that high temperature steam-water mixture rather than superheated steam is more favourable for hydrothermal crystallization. The reduced background level and the increase in intensity of the peaks with the decrease in steam to water ratio clearly indicates that presence of more water favours the crystallization of the amorphous powder. Further studies on this direction can't be performed because of the limitations of the quartz tubes in terms of strength.

There are two possible mechanisms, which have been proposed by various authors to explain the phenomenon of hydrothermal crystallization. These are (a) solution reprecipitation (b) topotactic nucleation. In the solution-reprecipitation mechanism, the amorphous precursor goes into solution and then reprecipitated in crystalline form. In the topotactic nucleation mechanism, it is assumed that the amorphous precursor has short-range order that resembles the crystalline phase, which grows in the surrounding amorphous matrix during the process of crystallization. Various authors have proposed the regions in which one or the mechanism is believed to dominate.

In order to throw some light on the mechanism operating during the hydrothermal crystallization we carried out various experiments. They are discussed below.

3.2.4 SEEDING EXPERIMENTS

A small amount of the previously crystallized powder was added as a seed to the amorphous gel powder. The amount of the seed material was 0.5%, 5%, and 50% by weight of the amorphous powder. The mixture was ultrasonicated for 10 minutes

before the hydrothermal treatment. The hydrothermal crystallization experiments were carried out at 320°C, 2MPa for 6 hours. Fig 3.2.8 gives the particle size

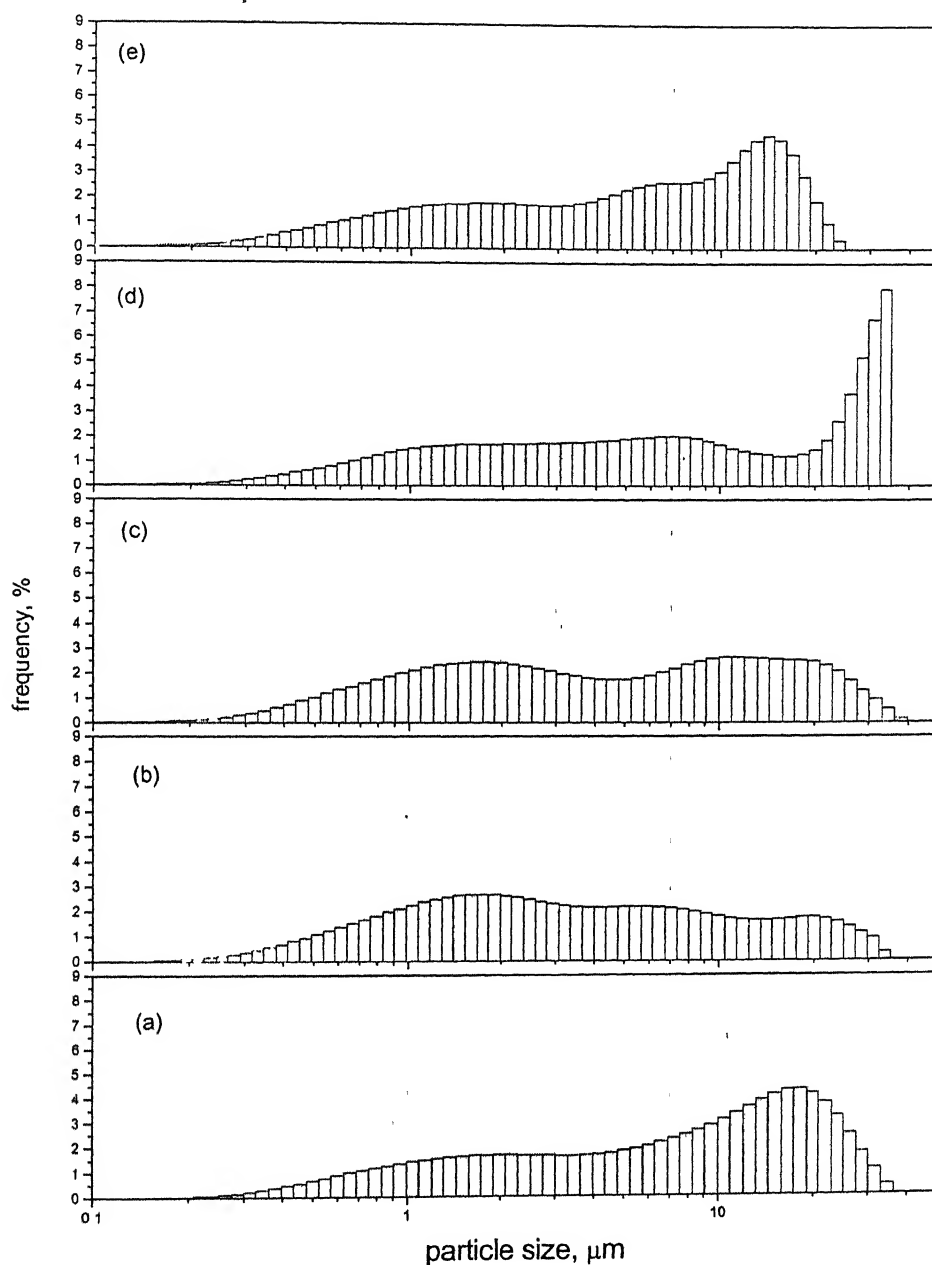


Figure 3.2.8 Particle size distribution of the powders seeded with different amount of crystalline material and hydrothermally crystallized at 320°C, 2MPa for 6 hours. The particle size distribution of the (a) amorphous powder and the (b) crystalline seed is given for comparison. (c) 0.5 % seeded, (d) 5 % seeded, (e) 50 % seeded

distribution of the resulting powders. The particle size distribution of the seed material and the starting amorphous powder are also given for comparison. The particle size distribution remains nearly unchanged in all the cases

In a repeat set of experiments done after several months similar trend was observed (figure 3.2.9) although in this case the seed material was found to have a narrower, nearly bell shaped distribution (figure 3.2.9a).

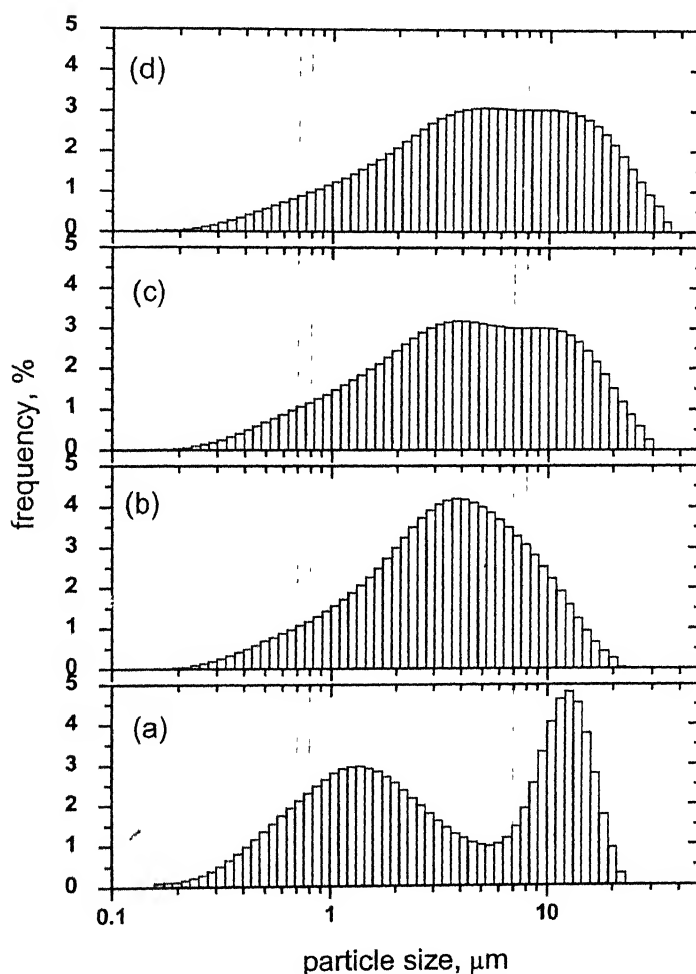


Figure 3.2.10. Particle size distribution of the powders seeded with different amount of crystalline material and hydrothermally crystallized at 320°C, 2MPa for 6 hours. The particle size distribution of the (a) amorphous powder and the (b) crystalline seed is given for comparison. (c) 0.5 % seeded, (d) 50 % seeded

Some seeded experiments were also carried out at 220°C, 1.6 MPa for 6 hours. Fig 3.2.10 shows the X-ray diffractograms of the powder using 5 weight percent seed at 320°C and 220°C. It is seen that the sample at 220°C is poorly crystallized while that treated at 320°C is fully crystallized. The experiment at 220°C was repeated several times and each time the crystallization was found to be incomplete. It should be noted that when no seed was added, complete crystallization was obtained even at 220°C [fig 3.2.1]. The reason for this is not clearly understood.

In order to further elucidate the mechanism of crystallization, the amorphous powder was fractionated by sedimentation into two fractions, one having particles less than 5 μm and the other having the particle size more than 5 μm . The hydrothermal crystallization was carried out as before at 320°C. The particle size distributions of

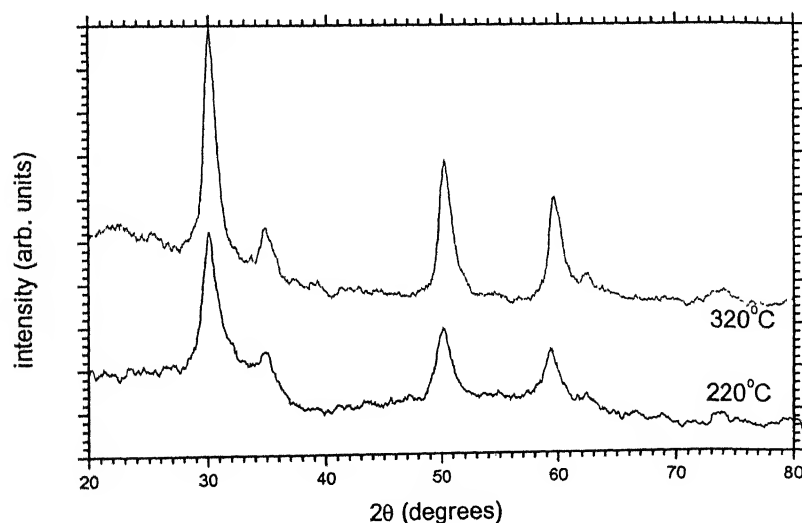


Figure 3.2.10. X-ray diffractograms of the powders hydrothermally crystallized with 5% seed material (prepared by hydrothermal crystallization at 320°C, 2MPa for 6 hours) for 6 hours at temperatures indicated in the figure

the starting powders and the products are shown in fig 3.2.11. It is seen that in the case of finer fraction the crystalline powder has an apparent bimodal distribution. However in this case the larger sized portion of the data is most probably an artifact arising due to the lens of the particle size analyser instrument not been cleaned. Similar artefacts were observed in all the successive runs of the instrument. If this artifact is ignored then the particle size of the distribution of the crystalline material is seen to be nearly identical to that of amorphous precursor material.

In the case when the starting fraction was very coarse, the particle size distribution of the crystalline material is distinctly different from that of the precursor material. The crystalline powder size is much smaller than that of the amorphous precursor. Such reduction in particle size was found in few other experiments also. However, in most cases the particle size of the crystalline product was found to be very similar to that of the starting amorphous powder.

To see if the ultrasonication of the reactants before hydrothermal treatment had any influence on the crystallization behaviour, the crystallization of the gel powder was carried out after ultrasonication of the suspension exactly in the same manner as was done for the seeded samples. The particle size distribution of the resulting crystalline powder is shown in fig 3.2.12. The figure shows that ultrasonication has no significant effect on the particle size of the crystallized powders.

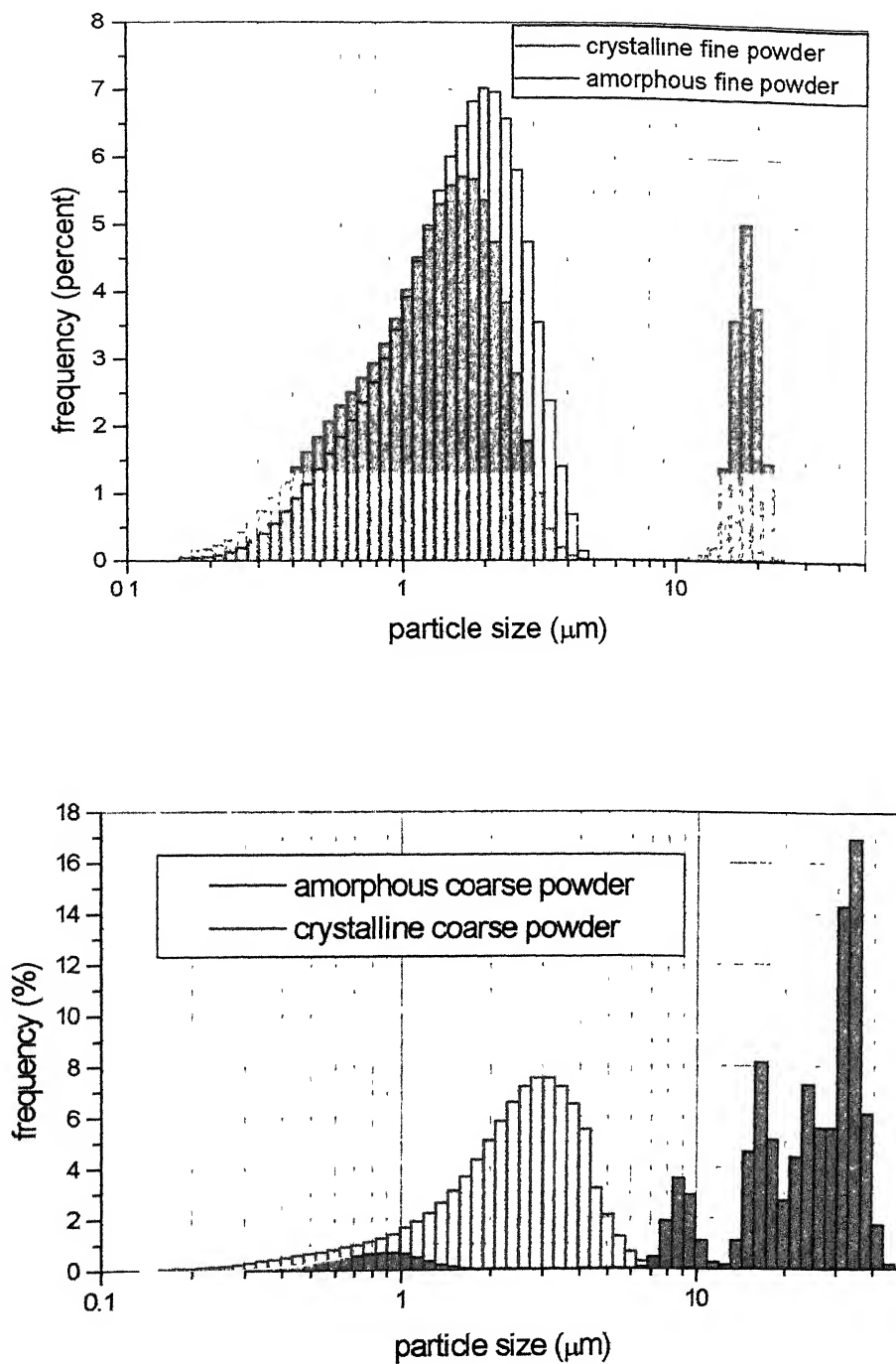


Fig 3.2.12. Particle size distribution of the amorphous powder and the powder hydrothermally crystallized form it at 320°C, 2 MPa for 6 hours: the starting particle sizes are different

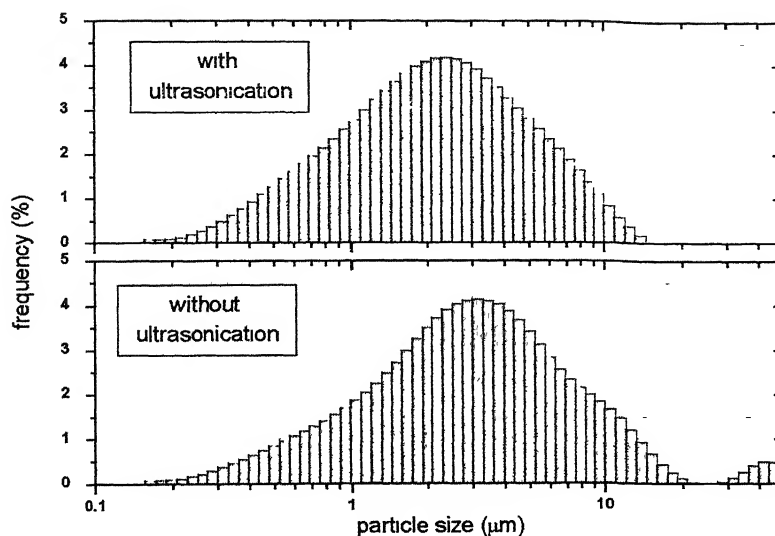


Figure 3.2.12. Particle size distribution of the powders hydrothermally crystallized at 320°C, 2 MPa for 6 hours with 10 minutes ultrasonication before hydrothermal treatment. Powders hydrothermally crystallized under similar conditions without ultrasonication is also shown for comparison.

As the particle size remains nearly identical, even after seeding it seems that the mechanism of hydrothermal crystallization is topotactic nucleation and growth. It has been reported that even in the amorphous powder there are some ordered regions of a few atomic distance that have the symmetry of the crystalline phase. Under suitable conditions these regions act as nuclei for the growth of the corresponding crystalline phase. The bonds around these nuclei rearrange themselves to form a ordered lattice.

Assuming that the growth of the crystalline particles occurs by addition of nanosized crystalline particles, it can be shown that the growth rate of the particle should depend inversely on the particle size. On the other hand, a solution reprecipitation mechanism of particle growth should lead to a shift of the whole particle size distribution towards larger particle size. None of these mechanisms seems to be operating during the hydrothermal crystallization as the hydrothermal crystallization of fine amorphous powder with a particle size $< 5\mu\text{m}$ doesn't show any growth of particle size or shift in the particle size distribution towards larger particle size. The crystallization of the amorphous phase is faster when hydrothermal treatment was done in high temperature steam water mixture compared to that in superheated steam. The idea of solution-reprecipitation mechanism fits this observation. However, further studies are required to confirm this hypothesis.

Though the mechanism of hydrothermal crystallization under the experimental conditions seems to be predominantly topotactic nucleation and growth, some observations suggest that the mechanism might not be a classical topotactic nucleation and growth, rather some variation of the topotactic mechanism. It is also possible that some other processes are operating simultaneously with topotactic nucleation and growth. The observations that contradict the idea of classical topotactic nucleation and growth mechanism are discussed below.

1. The hydrothermal crystallization process at low temperature, pressure (220°C , 1.6 MPa) seems to be retarded in presence of previously crystallized seed material. Had it been purely a topotactic crystallization mechanism the crystallization might not have affected by the presence of previously crystallized seed material.

2. In the hydrothermal seeding experiments, the particle size distribution of the crystalline seed material and the crystalline powder obtained after hydrothermal treatment of the seeded amorphous powder was nearly identical. However, in every case there is a little increase in the amount and size of the larger particle size fraction, which suggests there might be some growth process operating - either dissolution reprecipitation or addition of finer particles to the larger agglomerates. In contrary, when the larger particle size fraction of the amorphous powder was separated and hydrothermally treated the particle size distribution seems to decrease to lower sizes, indicating the breaking of the agglomerates instead of their growth. The reason for this not clearly understood.

Though, the crystallite size of the crystalline phase obtained by the hydrothermal crystallization of the amorphous powder is in the range of 20 to 50nm the particle size distribution ranges from 0.1 to 35 μ m. This shows that the particles are highly agglomerated and even ultrasonication was not sufficient to break the agglomeration. This also indirectly confirms the topotactic mechanism.

4

Conclusions

The major aim of the present study was to prepare gadolinia doped zirconia powder by urea hydrolysis and hydrothermal crystallization and to investigate the different aspects of hydrothermal crystallization. Such powder is difficult to prepare and only one report exists in which gadolinia-doped zirconia powders have been prepared by coprecipitation method using an alkoxide as the source of zirconium. In the present work it has been possible to prepare $\text{ZrO}_2\text{--Gd}_2\text{O}_3$ powders by hydrothermal crystallization using salts of zirconium and gadolinium as precursors. The conclusions drawn from the present investigation are as follows.

► Urea hydrolysis of a solution of zirconium oxychloride octahydrate and gadolinium nitrate followed by thorough washing with water and then by n-propanol and overnight drying at $\sim 80^\circ\text{C}$ produces ultra fine amorphous powder. Powders with compositions of 2, 5, 8, and 10 mole percent gadolinia were prepared. For $\text{ZrO}_2\text{--}10\%$

Gd₂O₃ powder, the surface area is 245 m²/gm which corresponds to an effective particle size of ~2nm assuming all the particles are spherical

► The amorphous powder crystallizes to monoclinic or cubic phases depending on composition when heated in a sealed quartz tube under a steam temperature as low as 220°C and pressure ~1.6 MPa for 6 hours. DI water (pH ~7) is used to create the steam pressure autogenously. Hydrothermal crystallization at such a low temperature, pressure and in the absence of any mineralizers (that would enhance the solubility of zirconia) has not been reported before.

► Hydrothermal crystallization at 270°C and ~1.8 MPa steam pressure yields pure cubic zirconia when the amorphous powders corresponding to the compositions ZrO₂ – 8 mole % Gd₂O₃ and ZrO₂ – 10 mole % Gd₂O₃ are treated for 6 hours. ZrO₂ – 2 mole % Gd₂O₃ powders crystallizes into pure monoclinic phase when heated under same conditions. These results are expected from ZrO₂ – Gd₂O₃ phase diagram. Surprisingly, the ZrO₂ – 5 mole % Gd₂O₃ powder crystallizes into monoclinic phase under similar conditions whereas from the results of Bhattacharya and Agrawal, this composition should yield mostly a tetragonal phase with a small amount of cubic phase.

► The crystallite size of the crystalline phase formed by hydrothermal treatment increases with hydrothermal temperature, pressure. Hydrothermal treatment of ZrO₂ – 10 mole % Gd₂O₃ powder yields pure cubic zirconia of crystallite size of ~27nm when treated at 220°C, 1.6 MPa for 6 hours and ~55nm when treated at 320°C, 2 MPa for 6 hours.

► The degree of crystallization during the hydrothermal treatment increases with pressure when the temperature and time are kept constant. Hydrothermal treatment of

ZrO₂–10mole % Gd₂O₃ powder at 220°C for 6 hours shows relatively more crystallization as the hydrothermal pressure is increased from 1.3 MPa to 2.1 MPa. The particle size also seems to decrease with increase in pressure as observed in scanning electron microscope.

► The particle size of the crystallized powder is lower on hydrothermal treatment in acidic pH. In the basic pH range the particle size seems to increase. The crystallite size as determined from the x-ray line broadening using Scherrer's formula, remains unchanged in all the cases at ~30nm except for the powders prepared at pH 3 when the crystallite size is 45nm. The reason for the increase in particle size (agglomeration) of the powders with pH is not very clear. Further studies are required to ascertain if at all solubility has any role to play in the variation of particle size as reported in the literature.

► At pH ~7 the mechanism of hydrothermal crystallization is principally topotactic nucleation and growth. The different results that support this mechanism are given below.

● Hydrothermal crystallization carried out at different temperatures, pressure conditions shows no significant change in the particle size distribution of the crystallized product from that of the amorphous powder. Solution-reprecipitation, the other proposed mechanism of hydrothermal crystallization, would lead to a shift in the particle size distribution of the amorphous powder to the higher ranges after hydrothermal treatment.

● Addition of previously crystallized powders as a seed material to the amorphous powder and hydrothermal treatment at 320°C and 2 MPa pressure for 6 hours produces no significant change in the particle size. If solution-reprecipitation were the mechanism the seeds would have grown to larger particle size. On the contrary, the

addition of these crystallized seed hinders the crystallization of the amorphous powders at lower temperature. The reason for this is not clearly understood.

- Hydrothermal crystallization of the amorphous powder with a particle size $< 5 \mu\text{m}$ at 320°C and 2 MPa pressure for 6 hours show no significant change in the particle size after the treatment. In one experiment, the hydrothermal crystallization of the coarser amorphous powder under similar conditions leads to a decrease in the particle size distribution. The result is to be confirmed.

- ▶ Hydrothermal crystallization in high temperature steam-water mixture rather than superheated steam seems to be more effective in crystallization. In 1:1 steam-water mixture at 220°C and 3.2 MPa pressure, complete crystallization can be obtained in 2 hours compared to 6 hours when hydrothermal crystallization was done at 220°C and 1.6 MPa pressure in superheated steam. Crystallization seems to be more effective when the steam water ratio is >1 . However further studies are required in this direction.

References

1. W. J. Dawson, "Hydrothermal Synthesis of Advanced Ceramic Powders," *Am. Ceram. Soc. Bul.*, **67** [10] 1673-1678 (1988).
2. G. W. Morey, "Hydrothermal Synthesis," *J. Am. Ceram. Soc.*, **36** [9] 279-285 (1953).
3. S. Somiya and T. Akiba, "Hydrothermal Zirconia Powder: A Review," *J. Eu. Ceram. Soc.*, **19** (1999) 81-87.
4. P. E. D. Morgan, "Synthesis of 6 nm Ultrafine Monoclinic Zirconia," *J. Am. Ceram. Soc.*, **67** [10] C204-205 (1984).
5. A. Bleier and R. M. Cannon, "Nucleation and Growth of Uniform m-ZrO₂," in *Better Ceramics Through Chemistry II, Proceedings of Materials Research Society*, vol. 73, edited by C. J. Brinker, D. E. Clark and D. R. Ulrich, Materials Research Society, PA 1986.
6. T. Sukuda, S. Venigalla, A. A. Marrone, J. H. Adair, "Low Temperature Hydrothermal Synthesis of Yttrium Doped Zirconia Powders," *J. Am. Ceram. Soc.*, **82** [5] 1169-1174 (1999).
7. G. Dell'Agli and G. Mascolo, "Hydrothermal Synthesis of ZrO₂ - Y₂O₃ Solid Solutions at Low Temperatures," *J. Eu. Ceram. Soc.*, **20** (2000) 139-145.
8. R. P. Denkwicz, K. S. TenHuisen, J. H. Adair, "Hydrothermal Crystallization Kinetics of m-ZrO₂ and t-ZrO₂," *J. Mater. Res.*, Vol 5 No. 11 Nov 1990.
9. J. H. Adair, R. P. Denkwicz and F. J. Arriagada, "Precipitation and In-situ Transformation in the Hydrothermal Synthesis of Crystalline Zirconium Oxide," in *Ceramic Powder Science II, A, Ceramic Transactions*, vol. 1, edited by G. L.

- Messing, E. R. Fuller, Jr, and H. Hausner, The American ceramic Society, Inc, Westerville, OH 1988
10. C. Hu-Min, W. Li-Jun, M. Ji-Ming, Z Zhi-Ying, Q. Li-Man, "The Effects of pH and Alkaline Earth Ions on The Formation of Nanosized Zirconia Phases Under Hydrothermal Conditions," *J. Eu. Ceram. Soc.*, **19** (1999) 1675-1681.
 11. H. Nashizawa, N. Yamashaki and K. Matusoka, "Crystallization and Transformation of Zirconia Under Hydrothermal Conditions," *J. Am. Ceram. Soc.*, **65** [7] 343-346 (1982).
 12. W. Pyda, K. Haberko, M. M. Bucko, "Hydrothermal Crystallization of Zirconia and Zirconia Solid Solutions," *J. Am. Ceram. Soc.*, **74** [10] 2622-2629 (1991).
 13. M. M. Bucko, K. Haberko, M. Faryna, "Crystallization of Zirconia Under Hydrothermal Conditions," *J. Am. Ceram. Soc.*, **78** [12] 3397-3400 (1995).
 14. M. M. Bucko and K. Haberko, "Mechanism of Hydrothermal Crystallization of Zirconia," *Key Engineering Materials*, vol. 132-136 (1997) p 121-124.
 15. E. Tani, M. Yoshimura, S. Somiya, "Formation of Ultrafine Zirconia Under Hydrothermal Conditions," *J. Am. Ceram. Soc.*, **66** [1] 11-14 (1983).
 16. E. Tani, M. Yoshimura, S. Somiya, "Hydrothermal Preparation of Ultrafine Monoclinic Zirconia Powders," *J. Am. Ceram. Soc.*, **64** [12] C181 (1981).
 17. M. Yoshimura, S. Somiya, "Fine Zirconia Powders by Hydrothermal Processing," *Report of the Research Laboratory of Engineering Materials, Tokyo Institute of Technology*, no. 9 (1984) 53-64.
 18. J. Livage, K. Doi, C. Mazieres, "Nature and Thermal Evolution of Amorphous Hydrated Zirconium Oxide," *J. Am. Ceram. Soc.*, **51** [6] 349-353 (1968).
 19. G. J. Burrows & C. E. Fawsuit, "The Decomposition of Carbamide," *J. Chem. Soc. (london)*, **105** 609 -623 (1914).
 20. E. A. Werner, "The constitution of carbamides Part V The Mechanism of Decomposition of Urea when Heated in Solution with Alkalis and with Acids

- respectively, the hydrolysis of Metallic Cyanate," *Zeitsch. Physikal. Chem.*, **113**, 84-99 (1918).
21. E. A. Werner, "The constitution of carbamides. Part XII. The Decomposition of Urea when Heated in Solution in presence with Acids," *Zeitsch. Physikal. Chem.*, **117**, 1078-81 (1920).
22. Walker and Wood, *Zeitsch. Physikal. Chem.*, **83**, 484 (1903).
23. W. H. R. Shaw and J. J. Bordeaux, "The Decomposition of Urea in Aqueous Media," *J. Am. Ceram. Soc.*, **77** 4729-4733 (1955).
24. H. Yeu-Xiang and G. Cunji, "Synthesis of Nanosized Zirconia via Urea Hydrolysis," *Powder Technology*, **72** 101-104 (1992).
25. M. J. Ready and D. W. Ready, "Sintering of ZrO_2 in HCl Atmosphere," *J. Am. Ceram. Soc.*, **69** [7] 580-582 (1986).
26. T. Suzuki, S. Osaka, and N. Aikawa, "Micronized Alumina and the Method for Production Thereof," Eur. Pat. Appl. 01717136A2, Feb19, 1986.
27. A. Roosen and H. Hausner, "The Influence of Processing Conditions on the Sintering Behavior of Coprecipitated Calcia Stabilized Zirconia Powders," pp 773-782 in *Ceramic Powder Materials Science Monographs*, **16**, Proceedings of the 5th International Meeting on Modern Ceramic Technologies (5th CIMITEC), Ligano Sabbiadaro, Italy, June 1982, edited by P. Vincenzini. Elsevier Scientific, 1983.
28. S. L. Jones and C. J. Norman, "Dehydration of Hydrous Zirconia with Methanol," *J. Am. Ceram. Soc.*, **71** [4] C-190 - C191 (1988).
29. M. J. Ready, R. R. Lee and J. W. Halloran, "Processing and Sintering of Ultrafine $MgO-ZrO_2$ and $(MgO, Y_2O_3)-ZrO_2$ Powders," *J. Am. Ceram. Soc.*, **73** [6] 1499-1503 (1986).
30. L. M. Zaitsev, "Zirconium Hydroxides," *Russ. J. Inorg. Chem. (Engl. Transl.)*, **11**, 900-904 (1968)

-
31. M. S. Kaliszewski and A. H. Heuer, "Alcohol Interaction with Zirconia Powders," *J. Am. Ceram. Soc.*, **73** [6] 1504 – 1509 (1990).
 32. Harold P. Klug and Leroy E. Alexander, *X-ray Diffraction Procedures for Polycrystalline and Amorphous Materials*, John Wiley & Sons Inc. 1974

A

141850



A1-1850